

HELMINTHOLOGIA, 60, 1: 1 - 27, 2023

Revision of *Corynosoma australe* Johnston, 1937 (Acanthocephala: Polymorphidae) from a North American population using novel SEM images, Energy Dispersive X-ray Analysis, and molecular analysis

O. M. AMIN^{1,*}, A. CHAUDHARY², H. S. SINGH^{2,3}, T. KUZMINA^{4,5}

¹Institute of Parasitic Diseases, 11445 E. Via Linda 2-419, Scottsdale, Arizona 85259, USA, Email: omaramin@aol.com; ²Molecular Taxonomy Laboratory, Department of Zoology, Chaudhary Charan Singh University, Meerut (U.P.), 250004, India; ³Vice Chancellor, Maa Shakumbhari University, Saharanpur (Uttar Pradesh), 247120, India; ⁴I. I. Schmalhausen Institute of Zoology NAS of Ukraine, Bogdan Khmelnytsky str., 15, Kyiv, 01030, Ukraine; ⁵Institute of Parasitology, Slovak Academy of Sciences, Košice, Slovak Republic

Article info

Received August 3, 2022
Accepted February 14, 2023

Summary

We describe a population of the acanthocephalan *Corynosoma australe* Johnston, 1937 (Polymorphidae) from a California sea lion *Zalophus californianus* (Lesson, 1828) in California using novel scanning electron microscopy (SEM) images, Energy Dispersive x-ray analysis (EDXA), and molecular analysis for the first time. The taxonomic history of *C. australe* is replete with accounts using only line drawings some of which proved erroneous. The distribution of ventral spines on the female trunk has been the primary distinction between *C. australe* and *Corynosoma obtuscens* Lincicome, 1943, its junior synonym; being continuous in the latter but discontinuous posteriorly in the former species. The distribution of ventral spines is invariably discontinuous in males. Our redescription and SEM images help to resolve this issue further validating the synonymy. Morphological variability has been documented between our California population and others from various host species in California, South Australia, South Shetlands, and the Argentinian coast. Our SEM images document features not previously detectable in line drawings, erroneously reported or missed in previous accounts. The EDXA spectra show high levels of calcium and phosphorous and low levels of sulfur characteristic of *C. australe*. EDXA for other species of *Corynosoma* Lühe, 1904 provide support for the diagnostic distinction of *C. australe*. EDXA spectra were shown to be species specific and have diagnostic value in the taxonomy of the Acanthocephala. Our molecular analysis used amplification of 18S of ribosomal DNA and cytochrome c oxidase 1 (Cox1) gene. Phylogenetic analyses for Cox1 gene revealed a close relationship between *Corynosoma hanna*e Zdzitowiecki, 1984 and *C. australe*. The phylogenetic trees confirmed that the isolates belonged to *C. australe*. The haplotype network inferred by Cox1 with *C. australe* sequences revealed that haplotypes clearly separated from each other and formed clusters related to samples from the Northern Hemisphere (the USA and Mexico), and the second from the Southern Hemisphere (Argentina, Brazil and Peru).

Keywords: *Corynosoma australe*; *Zalophus californianus*; redescription; molecular-profile

Introduction

The taxonomic literature of species of the genus *Corynosoma* Lühe, 1904 has been in flux, especially over the last few years with

the erection of the genus *Pseudocorynosoma* Aznar, Pérez-Ponce de León and Raga, 2006 for freshwater species formerly classified under *Corynosoma* (Aznar *et al.*, 2006; Garcia-Varela *et al.*, 2009; Amin, 2013). The history of *Corynosoma australe*, Johnston, 1937

* – corresponding author

originally described from an Australian sea lion *Neophoca cinerea* (Péron, 1816) with a host listing of the Australian hair seal *Arctocephalus forsteri* Lesson (Otaridae) off Pearson Island, South Australia, is less complex with its junior synonym *Corynosoma obtusens* Lincicome, 1943 being redescribed from the California sea lion *Zalophus californianus* (Lesson, 1828) in California. *Corynosoma otariae* Morini and Boero, 1958 from the South American sea lion, *Otaria flavescens* Shaw, 1800 in Argentina is also considered a junior synonym of *C. australe*. Various reports have since used the two names alternatively with *C. australe* being more commonly reported from the Southern Hemisphere and the junior synonym *C. obtusens* used along the Pacific coasts of North and South America (Van Cleave, 1953; Zdzitowiecki, 1984; Aznar *et al.*, 2012; Lisitsyna *et al.*, 2019). The confusion between these two entities was evident throughout the literature but the similarities were first noted by Johnston and Edmonds (1953) and later by Zdzitowiecki (1984). The differential distribution of ventral trunk spines in females was the primary distinguishing factor between the two species. More recently, Aznar *et al.* (2016) provided a scanning electron microscopy (SEM) study of trunk spine coverage in 6 species of *Corynosoma* from 5 species of marine mammals off Argentina including *C. australe* (N=10) from the South American sea lion, *O. flavescens*. Hernández-Orts *et al.* (2017a) reported on host switching in *C. australe* from Brazil, provided 4

SEM images of a male and female and their posterior trunk ends collected from the Magellanic penguin, *Spheniscus magellanicus* Forster 1781, and included Bayesian inference phylograms from 28SrRNA and *cox1* data sets. Some SEM images, dissimilar Energy Dispersive x-ray analysis (EDXA) from a different population of *C. australe* from the Cape fur seal, *Arctocephalus pusillus pusillus* (Schreber, 1775) off the Namibian coast, South Africa were provided by Halajian *et al.* (2020).

We have studied many species of acanthocephalans using X-ray scans (EDXA) of Focused Ion Beam (FIB)-sectioned hooks and spines for metal composition. The biological significance of EDXA as a diagnostic tool is exemplified by the observation that populations of acanthocephalan species will consistently have similar EDXA spectra irrespective of host species or geography (Amin *et al.*, 2022d). Results of the EDXA of the FIB-sectioned hooks (dual beam SEM) of *C. australe* show differential composition and distribution of metals in different hook parts characteristic of the species being examined.

A chronological history of the taxonomy of *C. australe* is listed in Table 1 emphasizing the variations in the distribution of ventral trunk spines in females. The present report and especially some SEM images explain, in part, the different interpretations of trunk spine distribution in females. The EDXA provides additional diagnostic support of the identity of *C. australe*. Previous studies showed

Table 1. Chronological taxonomic history of *Corynosoma australe* from marine mammals, with special reference to ventral trunk spines in females.

Author	Host	Locality	Described as	Stage	Ventral spines
Johnston (1937)	<i>Neophoca cinerea</i> (Péron)	South Australia	<i>C. australe</i>	Adults	Discontinuous
Lincicome (1943)	<i>Zalophus californianus</i> (Lesson)	San Diego, California	<i>C. obtusens</i>	Adults	Continuous
Van Cleave (1953)	<i>Mycteroperca pardalis</i> Gilbert	Mazatalán, Mexico	<i>C. obtusens</i>	Cystacanth	Continuous
Morini & Boero (1960)	<i>Otaria flavescens</i> Shaw	Argentina	<i>C. otariae</i>	Adults	Discontinuous
Zdzitowiecki (1984)	<i>Hydrurga leptonyx</i> (Blainville)	South Shetlands, Antarctica	<i>C. australe</i>	Adults	25% continuous
Smales (1986)	<i>Neophoca cinerea</i> (Péron) <i>Arctocephalus pusillatus</i> Schreber	South Australia	<i>C. australe</i>	Adults (Figs. 10,11)	Discontinuous
Zdzitowiecki (1991)	Few "suitable" definitive & paratenic hosts	Antarctica	<i>C. australe</i>	Adults (Figs. 15 b, e)	Discontinuous
Sardella <i>et al.</i> (2005)	<i>Arctocephalus australis</i> (Zimmerman) <i>Mirounga leonina</i> (Linn.) <i>Cynoscion guatucupa</i> (Cuvier)	Argentina	<i>C. australe</i> <i>C. australe</i> <i>C. australe</i>	Adults Adults Cystacanths	85–100% continuous 85–100% continuous 85–89% continuous
Aznar <i>et al.</i> (2012)	<i>Otaria flavescens</i> (Shaw)	Argentina	<i>C. australe</i>	Adults (Fig. 1B)	Discontinuous
Hernández-Orts <i>et al.</i> (2017a)	<i>Spheniscus magellanicus</i> (Foster)	Brazil	<i>C. australe</i>	Adults (Fig. 2B) Adults (Fig. 4B)	Continuous & 82–89% continuous
Lisitsyna <i>et al.</i> (2018)	<i>Zalophus californianus</i> (Lesson)	Sausalito California	<i>C. obtusens</i>	Adults	Continuous
Lisitsyna <i>et al.</i> (2019)	<i>Zalophus californianus</i> (Lesson)	Sausalito California	<i>C. obtusens</i> & <i>C. australe</i>	Adults	1% discontinuous
Present paper	<i>Zalophus californianus</i> (Lesson)	Sausalito California	<i>C. australe</i>	Adults	Continuous with post. constriction

that species delineation within the genus *Corynosoma* has been problematic for a long time (Sardella *et al.*, 2005; Hernández-Orts *et al.*, 2017a). Additionally, Stryukov (2004) also pointed out that heteropolar geographical distribution can be represented by the species that are similar in their morphology. Therefore, we carried out phylogenetic analyses using newly generated sequences of 18S ribosomal RNA and the mitochondrial cytochrome c oxidase subunit 1 (Cox1) gene that provide insights of the relationships of *C. australe* studied at the generic level and about their heteropolar geographical distribution.

Materials and Methods

Collections

Thirty-three sea lions, *Zalophus californianus* found stranded on the Pacific coast near San Francisco, California (37°46' N; 122°25' W) in February and March 2012, 2015 and 2016 were kept alive and subsequently died and examined for parasites in the Marine Mammal Center (TMMC), Sausalito, California (see Kuzmina *et al.*, 2018 for details). A total of 1,201 adult specimens of *C. australe* were collected from one 2-year-old female sea lion, necropsied at TMMC in 2015 (Lisitsyna *et al.*, 2018). Fifty-one specimens of this collection were whole mounted and studied by Lisitsyna *et al.* (2019) to verify the synonymy of *C. obtuscens* with *C. australe*. A sub-set of about 170 specimens from the initial larger collection was made available to Omar M. Amin (OMA) for our study. Of these specimens, 29 specimens were processed for microscopical studies, 12 for SEM, and 2 for molecular analysis. Twelve of the whole-mounted specimens were deposited at the Harold W. Manter Laboratory (HWML) parasitology collection,

University of Nebraska State Museum, Lincoln, Nebraska. The remaining specimens are in the OMA collection.

Methods for microscopical studies

Worms were punctured with a fine needle and subsequently stained in Mayer's acid carmine, destained in 4 % hydrochloric acid in 70 % ethanol, dehydrated in ascending concentrations of ethanol (24 hr each), and cleared in 100 % xylene then in 50 % Canada balsam and 50 % xylene (24 hr each). Whole worms were then mounted in Canada balsam. Measurements are in micrometers, unless otherwise noted; the range is followed by the mean values between parentheses. Width measurements represent maximum width. Trunk length does not include proboscis, neck, or bursa.

Line drawings

Line drawings were created by using a Ken-A-Vision micro projector (Ward's Biological Supply Co., Rochester, N.Y.) which uses cool quartz iodine 150W illumination. Images of stained whole mounted specimens are projected vertically on 300 series Bristol draft paper (Starthmore, Westfield, Massachusetts), then traced and inked with India ink. The completed line drawings are subsequently scanned at 600 pixels on a USB and subsequently downloaded on a computer.

Specimens

Voucher specimens were deposited at the University of Nebraska's State Museum Harold W. Manter Laboratory (HWML) collection in Lincoln, Nebraska, USA; No. 216825 (12 voucher specimens on 3 slides)

Table 2. List of acanthocephalan species used for phylogenetic analysis based on the 18S rDNA gene sequences. Newly generated sequences are presented in bold, NA=host name not available.

Species	Host	Host origin	GenBank accession nos.	References
<i>Corynosoma australe</i>	<i>Zalophus californianus</i>	USA	ON614192, ON614199	present study
	<i>Zalophus californianus</i>	USA	MK119255	Lisitsyna <i>et al.</i> , 2019
	<i>Phocarcos hookeri</i>	Mexico	JX442168	García-Varela <i>et al.</i> , 2013
<i>Corynosoma obtuscens</i>	<i>Callorhinus ursinus</i>	Mexico	JX442169	García-Varela <i>et al.</i> , 2013
<i>Corynosoma validum</i>	<i>Callorhinus ursinus</i>	Mexico	JX442170	García-Varela <i>et al.</i> , 2013
<i>Corynosoma enhydri</i>	NA	USA	AF001837	Near <i>et al.</i> , 1998
<i>Corynosoma magdaleni</i>	<i>Phoca hispida botnica</i>	Mexico	EU267803	García-Varela <i>et al.</i> , 2009
<i>Corynosoma strumosum</i>	<i>Phoca vitulina</i>	Mexico	EU267804	García-Varela <i>et al.</i> , 2009
<i>Bolbosoma balaenae</i>	<i>Nyctiphanes couchii</i>	Spain	JQ040306	Gregory <i>et al.</i> , 2011*
<i>Bolbosoma turbinella</i>	<i>Eschrichtius robustus</i>	Mexico	JX442166	García-Varela <i>et al.</i> , 2013
<i>Bolbosoma vasculosum</i>	<i>Lepturacanthus savala</i>	Indonesia	JX014225	Verweyen <i>et al.</i> , 2011
<i>Andracantha gravaida</i>	<i>Phalacrocorax auritus</i>	Mexico	EU267802	García-Varela <i>et al.</i> , 2009
<i>Hexaglandula corynosoma</i>	<i>Nyctanassa violacea</i>	Mexico	EU267808	García-Varela <i>et al.</i> , 2009
<i>Pseudocorynosoma anatarium</i>	<i>Bucephala albeola</i>	Mexico	EU267801	García-Varela <i>et al.</i> , 2009
<i>Pseudocorynosoma constrictum</i>	<i>Anas clypeata</i>	Mexico	EU267800	García-Varela <i>et al.</i> , 2009
<i>Profilicollis bullocki</i>	<i>Emerita analoga</i>	Mexico	JX442174	García-Varela <i>et al.</i> , 2013
<i>Profilicollis botulus</i>	<i>Somateria mollissima</i>	Mexico	EU267805	García-Varela <i>et al.</i> , 2009
<i>Polymorphus trochus</i>	<i>Fulica americana</i>	Mexico	JX442196	García-Varela <i>et al.</i> , 2013

* – direct submission of unpublished data to GenBank

were sectioned using the FEI Helios Dual Beam Nanolab mentioned above. A gas injection magnetron sputtering technique regulating the rate of cutting. The hooks of the acanthocephalans were centered on the SEM stage and cross-sectioned using an ion-accelerating voltage of 30 kV and a probe current of 2.7 nA following the initial cut. The sample goes through a cleaning cross-section milling process to obtain a smoother surface. The cut was analyzed with an X-ray normally at the tip, middle, and base of hooks for chemical ions with an electron beam (Tungsten) to obtain an X-ray spectrum. The intensity of the GIS was variable according to the nature of the material being cut. Results were stored with the attached imaging software and then transferred to a USB for future use.

Energy Dispersive X-Ray analysis (EDXA)

The Helios Nanolab 600 is equipped with an EDXA (Mahwah, NJ) TEAM Pegasus system with an Octane Plus detector. The sectioned cuts were analyzed by EDXA. Spectra of selected areas were collected from the center and the edge of each cross-section. EDXA spectra were collected using an accelerating voltage of 15 kV, and a probe current of 1.4 nA. Data collected included images of the displayed spectra as well as the raw collected data. Relative elemental percentages were generated by the TEAM software.

Molecular analyses

DNA extraction from ethanol-fixed specimens of *C. australe* (n=2) was performed using the DNeasy Blood & Tissue Kit (QIAGEN, Hilden, Germany) following the manufacturer's instructions. Sequences of the 18S rDNA and mitochondrial *cox1* gene were obtained by sequencing PCR products. For 18S we used the primers 18SU467F and 18SL1310R (Suzuki *et al.*, 2008) and PCR conditions according to Amin *et al.* (2022a). For *cox1*, we used the primers LCO1490 and HCO2198 (Folmer *et al.*, 1994) and PCR conditions as described by Amin *et al.* (2022a). PCR products were electrophoresed and purified with the Purelink™ PCR Purification Kit (Invitrogen). Sequencing was then performed in both directions with the same primers mentioned above using the Big Dye Terminator Cycle Sequencing Reaction Kit.

The sequences obtained were edited in BioEdit software (Hall, 1999) and aligned using ClustalW implemented in MEGA v.11 (Tamura *et al.*, 2021). List of acanthocephalans used in the phylogenetic analyses is presented in Tables 2 and 3. The best nucleotide substitution model was determined for 18S (GTR + I + G) and Cox1 (HKY+G+I) based on Akaike Information Criterion in MEGA MEGA v.11 (Tamura *et al.*, 2021). Phylogenetic analyses were performed using Maximum Likelihood (ML) and Bayesian inference (BI) methods. ML tree was computed in MEGA v.11 and 1000 bootstrap pseudoreplicates were estimated for nodal support. The BI analysis was performed in TOPALi software (Milne *et al.*, 2009) using Markov chain Monte Carlo (MCMC) searches on two simultaneous runs of four chains for 1,000,000 generations and sampling every 100th generation. The first 25 % of the sampled trees

were discarded as 'burn-in'. Information on the sequences used in the phylogenetic analyses is presented in Table 2. Pairwise genetic distances (uncorrected p-distance model) were calculated in MEGA v. 11. The new sequences obtained for *C. australe* in the present study were deposited in GenBank.

Among the populations of *C. australe*, we examined Cox1 haplotype frequency using the DNAsp v5 program (Librado & Rozas, 2009) and calculated the number of haplotypes (H) and the haplotype diversity (Hd). The haplotype network was constructed using Network software 10.2.0.0 version (Bandelt *et al.*, 1999).

Ethical Approval and/or Informed Consent

The authors declare that they have observed all applicable ethical standards.

Results

Of the 1,201 specimens originally collected from the single sea lion in California in 2015, 51 specimens (24 males, 27 females) were initially reported as *C. obtuscens* (Lisitsyna *et al.*, 2018; Kuzmina *et al.*, 2018) and re-identified as *C. australe* by Lisitsyna *et al.* (2019) and studied for morphological variability and morphometric comparisons. See Table 1 for hosts. Measurements of our subset of 29 specimens (16 males, 13 females) of the same collection were comparable to those of the 51 specimens reported by Lisitsyna *et al.* (2019, Table 2) from the same original collection from the same single sea lion. Lisitsyna *et al.* (2019) did not provide a qualitative description of the California specimens but included schematic line drawings of the outline of a whole male and a female (Figs. 1, 2) and photomicrographs of the posterior body wall of type females of *C. obtuscens* (Figs. 3 – 8).

In this presentation, we provide (1) a qualitative description of the California population of *C. australe*; (2) additional measurements and counts not available in Lisitsyna *et al.* (2019, Table 2) including dimensions of neck, lemnisci, cement glands, bursa, and length of the anterior, middle, and posterior hooks, and of the female reproductive system, and numbers of genital spines; (3) a complete set of SEM images now available for the first time, with noted exceptions (see below), depicting features not previously described or impossible to delineate using light microscopy and line drawing. Aznar *et al.* (2016) provided elaborate SEM of trunk spines. Hernández-Orts *et al.* (2017a) provided 4 SEM images of a male and a female and their posterior trunk. Halajian *et al.* (2020) provided a limited number of good quality SEM images missing whole male and female, anterior, middle and posterior hooks, sections of anterior, middle and posterior spines, detail and sensory structures of a male bursa, differentiation of micropores in various trunk regions, distribution of trunk spines in females; (4) a detailed EDXA of hook, spine, and egg spectra that shows notable differences from the pattern in a different population of *C. australe* from the Cape fur seal *Arctocephalus pusillus pusillus* in South Africa.

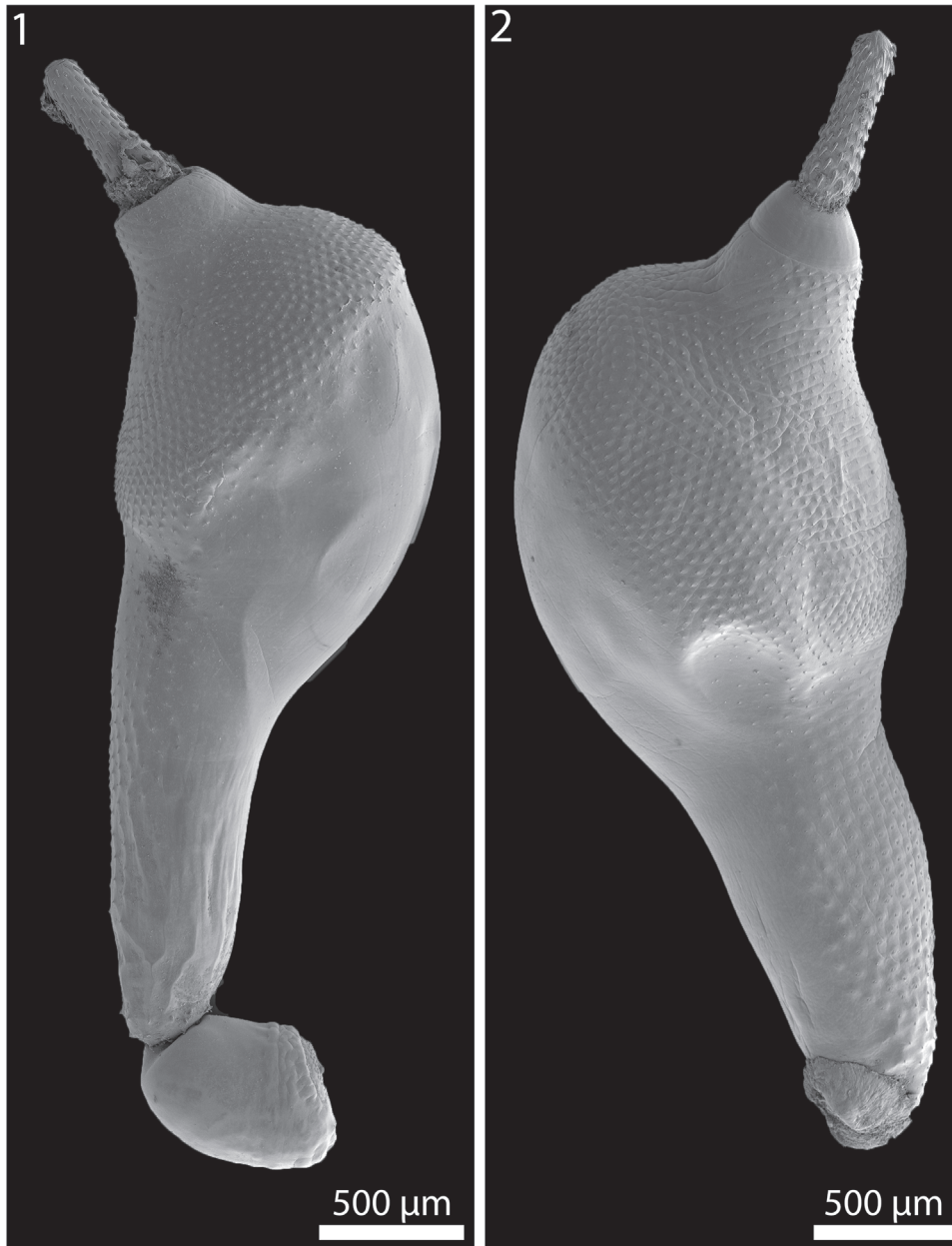
Scanning electron microscopy (SEM)

Twelve specimens that had been fixed and stored in 70 % ethanol were processed for SEM following standard methods (Lee, 1992) These included critical point drying (CPD) (Tousimis Automandri 931.GL) and mounting on aluminium SEM sample mounts (stubs) using conductive double-sided carbon tape. Samples were sputter coated with an 80 % – 20 % gold-palladium target for 3 minutes using a sputter coater (Quorum (Q150T ES) www.quorumtech.com) equipped with a planetary stage, depositing an approximate

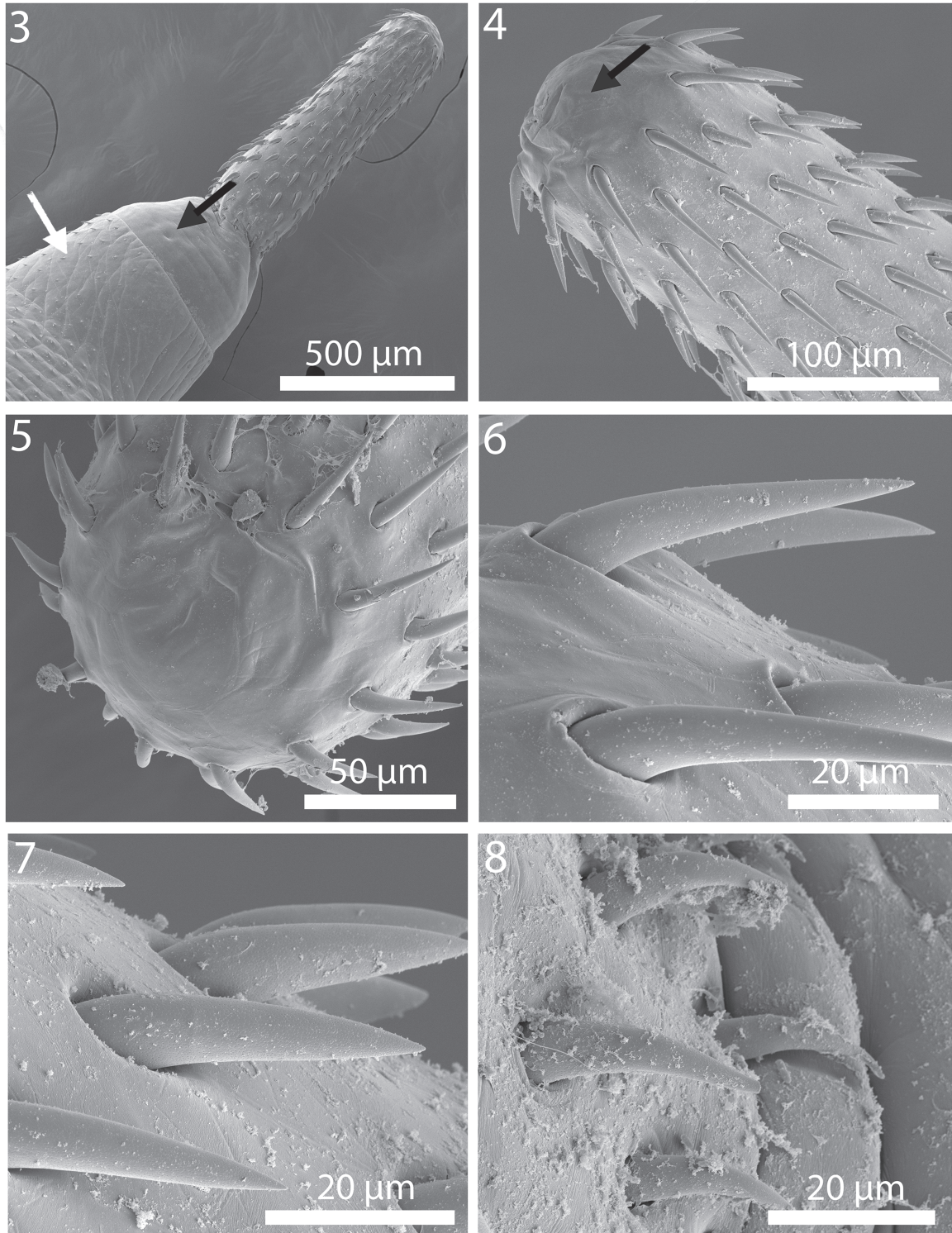
thickness of 20 nm. Samples were placed and observed in an FEI Helios Dual Beam Nanolab 600 (FEI, Hillsboro, Oregon) Scanning Electron Microscope (FEI, Hillsboro, Oregon). Samples were imaged using an accelerating voltage of 5 kV, and a probe current of 86 pA, at high vacuum using a SE detector.

Focused Ion Beam (FIB) sectioning of hooks

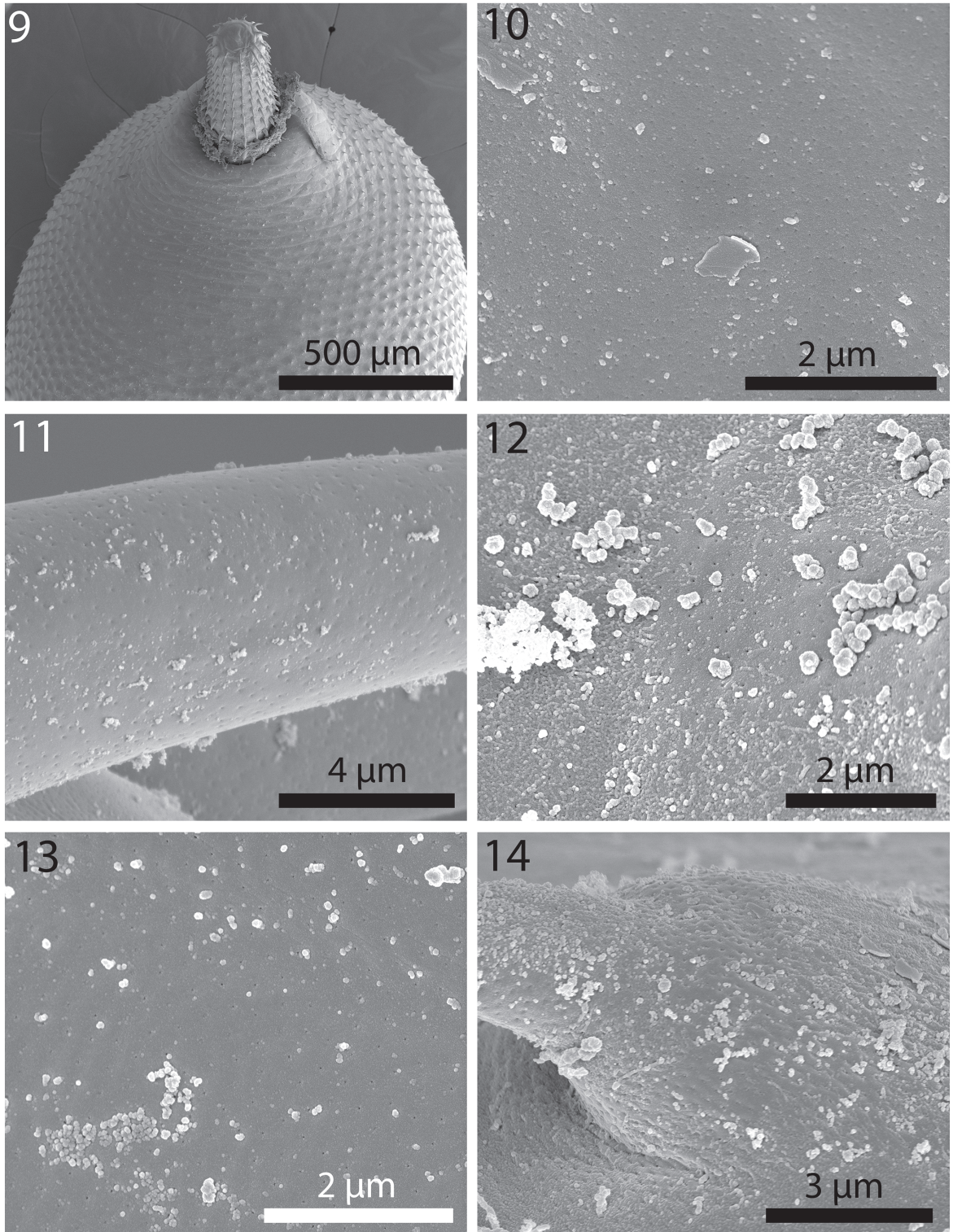
A dual-beam SEM with gallium (Ga) ion source (GIS) is used for the LIMS (Liquid Ion Metal Source) part of the process. Hooks



Figs. 1, 2. SEM of whole male (Fig. 1) and female (Fig. 2) specimens of *Corynosoma australe* from the intestines of *Zalophus californianus* in California. Note the continuity of the ventral field of spines from the neck to the genital area in the female which is covered with a copulation plug (Fig. 2).



Figs. 3–8. SEM of male and female specimens of *Corynosoma australe* from the intestines of *Zalophus californianus* in California. 3. Praesoma of a male worm showing the conical neck and the ventral spinose part of the anterior part of the trunk just anterior to the bulbus (white arrow) and the sensory pore (black arrow). 4. The anterior proboscis of a specimen showing the organization of the longitudinal rows of large hooks and the external appearance of the apical organ (arrow). 5. Apical view of the proboscis in Fig. 4 showing the external surface of the apical organ. 6. Lateral view of apical and subapical hooks. 7. Lateral view of middle hooks. 8. Posterior-most spine-like hooks. Note their arched curvature compared to more anterior hooks.



Figs. 9–14. SEM of anterior bulbus and micropores of male and female specimens of *Corynosoma australe* from the intestines of *Zalophus californianus* in California. 9. Antero-ventral view of the proboscis and bulbus of a female specimen. 10. Micropores at the anterior end of a proboscis. 11. Micropores on an anterior proboscis hook. 12. Micropores on anterior trunk spine. 13. Micropores at anterior end of a male trunk away from spines. 14. Micropores on the base of a posterior trunk spine in a male specimen.

(Halajian *et al.*, 2020), and (5) phylogenetic reconstruction using mt Cox1 sequences, a median-joining haplotype networks based on Cox1 sequence data of *C. australe* and a phylogenetic tree from Maximum likelihood and Bayesian inference analysis of the Cox1 sequences for our California material.

Of the taxonomic accounts listed in Table 1, only Smales (1986) provided a redescription of *C. australe* from *Neophoca cinerea* in South Australia that included a few qualified differences noted following. Zdzitowiecki (1984) also provided a detailed redescription of *C. australe* from pinnipeds which, however, included differences in the interpretation of the female reproductive system; see our Fig. 36 and corrections in Figs. 33, 34, and associated text. Lisitsyna *et al.* (2019) included an analysis for species of *Corynosoma* based on *cox 1* and 18S sequences. The following description is based on 29 specimens from *Zalophus californianus* in California. Characters reported for the first time are **bolded**.

Description

General. With characters of the genus *Corynosoma* Lühe, 1904 (Polymorphidae). Worms small, spindle-shaped, **with main longitudinal lacunar canals lateral, lemniscal, cement gland, and hypodermal nuclei fragmented, and ligament sacs in females single, not persistent**. Worms with slight sexual dimorphism in size of trunk, proboscis, hooks, and other structures in common (Figs. 1, 2). Praesoma, proboscis, and anterior receptacle bent ventrad. Swollen fore-trunk tapers gradually to more cylindrical hind-trunk. **About 6 – 8 incomplete circles of ventro-lateral spines just posterior to neck (Fig. 3) preceding complete compact circles of anterior trunk spines (crown spines)** extending posteriorly to area of maximum diameter of swollen fore-trunk dorsally in both sexes (Fig. 9). Ventral extension of spines between neck and the larger genital trunk spines continuous in females (Fig. 2) but invariably interrupted posteriorly in males (Fig. 1). Distribution of ventral spines from neck to genital spines (Fig. 18) not homogeneous. **Ventral space between crown spines (Figs. 9, 15) and spines on posterior cylindrical part of trunk (Fig. 17) occupied by smaller, weaker, and more thinly distributed transitional spines (Fig. 16; arrow) varying significantly in their size (smaller) and metal composition (poorer) using EDXA than other spines (Table 4). See differences in anatomy, size and strength of anterior, transitional and posterior trunk spines (Figs. 22 – 24, respectively). Continuous field of ventral trunk spines in females constricts posteriorly (Figs. 18 – 19, arrows) but never interrupted**. Genital spines most robust (Figs. 20 and 25). **Electron-dense micropores cover cuticular surfaces of anterior proboscis, hooks, spines, and aspinose areas of trunk (Figs. 10 – 14). See higher magnification of micropores on posterior and anterior trunk spines (Figs. 14 and 21, respectively). Proboscis long, cylindrical, slightly widening posteriorly, with elevated apical disc suggestive of surface of apical organ anteriorly (Figs. 4 – 5) and 17 – 19 longitudinal alternating rows of 11 – 14 hooks each. Hooks of 3 types. First type: anterior 7 – 9**

hooks almost equally long and most slender anteriorly, with posteriorly directed, simple roots shorter than blades especially apical and subapical hooks (Figs. 6, 35 AH). Second type: Posterior 2 or 3 hooks as long as anterior hooks but more robust and wider at base with posteriorly directed roots longer than blades (Figs. 7, 35 PH). **Third type: posterior-most 2 – 4 hooks (Figs. 8, 35 BH) smallest, curving, with shorter but distinct roots directed anteriorly (manubria). Neck conical with paired lateral sensory pores (Fig. 3, black arrow)**. Proboscis receptacle double-walled with cerebral ganglion about halfway at middle. Lemnisci equal, broad, rounded to irregular, shorter than receptacle.

Males. Based on 16 sexually mature adults with sperm. See Lisitsyna *et al.* (2019) for measurements and see additional measurements listed below. Apical, middle and basal hooks 37 – 47 (43), 40 – 45 (43), and 20 – 28 (25) long, respectively. Hook roots 30 – 37 (28), 40 – 47 (43), 15 – 22 (19), in the same order. Neck 157 – 218 (197) long by 333 – 395 (363) wide. Lemnisci 464 – 724 (602) long by 214 – 412 (325) wide. **Genital spine 20 – 32 (25) in 3 – 4 circles. Reproductive system in all trunk space posterior to level of mid-receptacle**. Testes relatively large, rounded, usually equal, crowded diagonally or laterally. Six pyriform **cement glands**, 300 – 522 (419) long by 187 – 270 (220) wide, in 3 pairs **contiguous with testes, with long ducts joining 2 common cement gland ducts overlapping claviform Saeftigen's pouch, all draining into terminal genital terminalia in bursa. Bursa muscular, large, longer than wide, 364 – 800 (570) long by 364 – 605 (433) wide, with slightly undulating lip (Figs. 25, 26), and with inner plump interface studded with 2 sets of sensory papillae. Central inner set of large round papillae encircled by many rings of complex, and less elevated papillae (Figs. 27, 28) at the outer edge of which flat-headed penis (Figs. 28, 29) is found**.

Females. Based on 13 gravid females with many eggs. See Lisitsyna *et al.* (2019) for measurements and see additional measurements below. Apical, middle, and basal hooks 42 – 50 (47), 45 – 50 (48), and 22 – 31 (27) long, respectively. Hook roots 35 – 47 (41), 45 – 57 (50), 20 – 27 (24) in the same order. Neck 166 – 260 (216) long by 343 – 437 (391) wide. **Genital spines 8 – 16 in 1 – 2 circles**. Lemnisci obscured by eggs. **Gonopore dorso-subterminal (Fig. 30) leading anteriorly to vaginal orifice, double sphincters, very long muscular uterus in 2 parts; lower and upper uterus joined by uterine bell cells (selective apparatus; SA) near its mid-point, then uterine bell adhering to ventral body wall (Figs. 33, 34). Reproductive system measuring 2.43 – 2.44 mm in two 3.45 mm long females not congested with eggs, (70 % of trunk length). Other length measurements: vagina 186 – 189, lower uterus 707 – 718, selector apparatus 177 – 225, upper uterus 1,021 – 1,040, uterine bell 300 – 312, and width measurements: selector apparatus 146 – 156, and uterine bell 208 – 215. Lower uterus inflated anteriorly irre-**

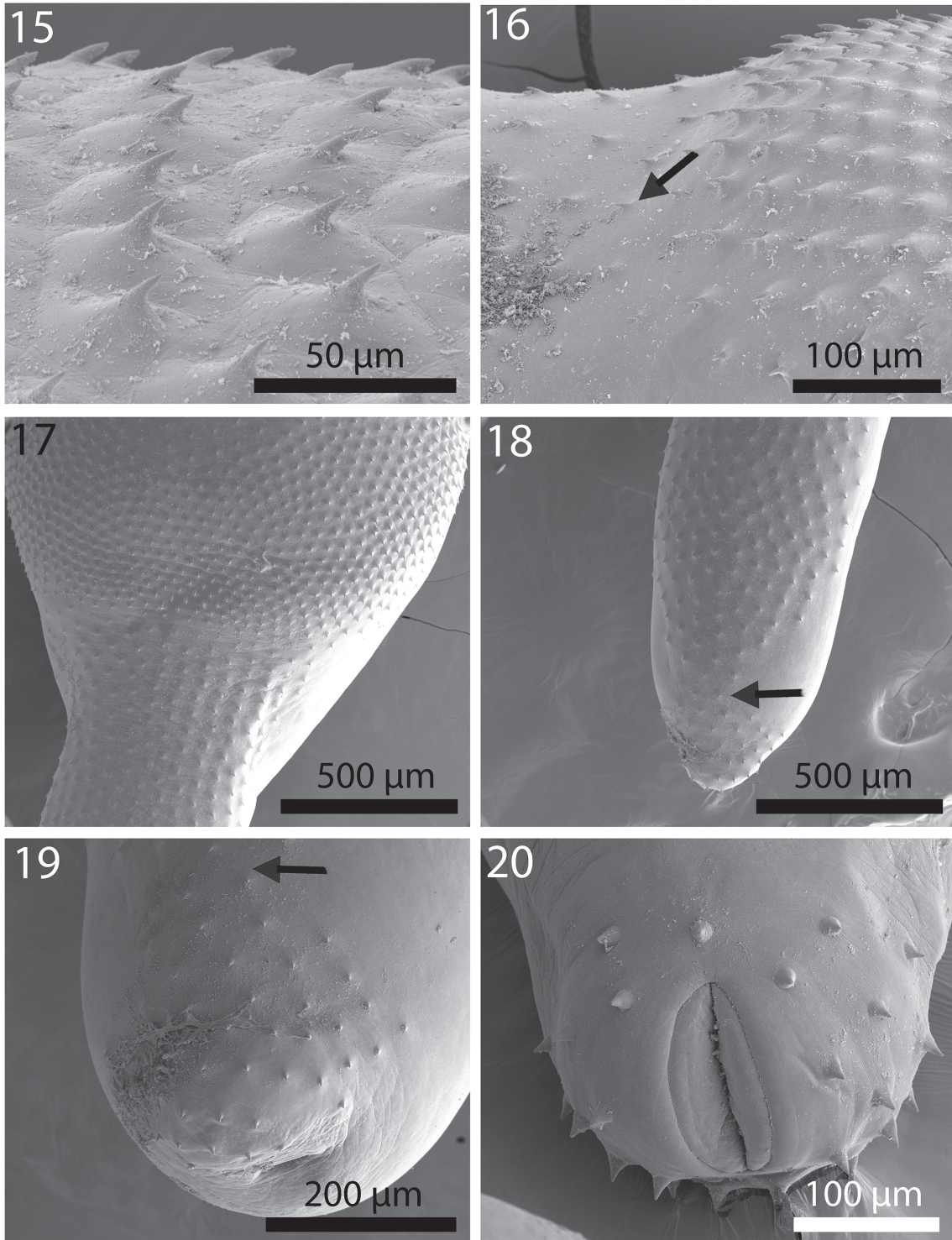
spective of presence or absence of eggs in it (Figs. 33, 34). Para-vaginal muscular sheet wrapping around vagina and lining posterior tip of trunk, particularly prominent ventrally. Four para-vaginal ligament cords, short and long ones each dorsally and ventrally, originating from posterior body wall and

vaginal interface dorsally and ventrally and extending anteriorly. Short cords insert in body wall just anterior to posterior tubular trunk region (para-vaginal-body wall ligament cords). Long cords reaching to base and side of uterine bell (para-vaginal-uterine-bell ligament cords) (Fig. 33). Eggs elliptic, oblong,

Table 3. List of acanthocephalan species used for phylogenetic analysis based on the mt Cox1 gene sequences. Newly generated sequences are presented in bold.

Species	Host	Host origin	GenBank accession nos.	References
<i>Corynosoma australe</i>	<i>Zalophus californianus</i>	USA	ON619618, ON614719	present study
	<i>Zalophus californianus</i>	USA	MK119245–MK119249	Lisitsyna <i>et al.</i> , 2019
	<i>Zalophus californianus</i>	Mexico	MT676808–MT676818	García-Varela <i>et al.</i> , 2020
	<i>Merluccius hubbsi</i>	Argentina	MT676819–MT676822	García-Varela <i>et al.</i> , 2020
	<i>Raneya brasiliensis</i>	Argentina	MT676823–MT676824	García-Varela <i>et al.</i> , 2020
	<i>Paralichthys isosceles</i>	Brazil	KU314822	Fonseca <i>et al.</i> , 2019
	<i>Stenella clymene</i>	Argentina	MW724483	Hernández-Orts <i>et al.</i> , 2021
	<i>Arctocephalus australis</i>	Argentina	MF497333	Hernández-Orts <i>et al.</i> , 2017a
	<i>Spheniscus magellanicus</i>	Brazil	MF497335	Hernández-Orts <i>et al.</i> , 2017a
	<i>Otaria flavescens</i>	Argentina	KX957714, MF497334	Hernández-Orts <i>et al.</i> , 2017a, b
	<i>Paralichthys adspersus</i>	Peru	MZ920052–MZ920055	Mondragon-Martinez <i>et al.</i> , 2021*
	<i>Paralabrax humeralis</i>	Peru	MZ920056–MZ920059	Mondragon-Martinez <i>et al.</i> , 2021*
	<i>Cheilodactylus variegatus</i>	Peru	MZ920060–MZ920063	Mondragon-Martinez <i>et al.</i> , 2021*
	<i>Otaria byronia</i>	Peru	MZ920064–MZ920067	Mondragon-Martinez <i>et al.</i> , 2021*
<i>Corynosoma hanna</i>	<i>Colistium guntheri</i>	New Zealand	KX957724, KX957725	Hernández-Orts <i>et al.</i> , 2017b
	<i>Leucocarbo chalconotus</i>	New Zealand	KX957718–KX957721, KX957723	Hernández-Orts <i>et al.</i> , 2017b
	<i>Phalacrocorax punctatus</i>	New Zealand	KX957722	Hernández-Orts <i>et al.</i> , 2017b
	<i>Phocarctos hookeri</i>	New Zealand	KX957715–KX957717, JX442191	Hernández-Orts <i>et al.</i> , 2017b; García-Varela <i>et al.</i> , 2013
	<i>Peltorhamphus novaezeelandiae</i>	New Zealand	KY909260–KY909263	Anglade & Randhawa, 2018
	<i>Halichoerus grypus</i>	Germany	MF001277	Waindok <i>et al.</i> , 2018
<i>Corynosoma semerme</i>	<i>Callorhinus ursinus</i>	USA	MK119253	Lisitsyna <i>et al.</i> , 2019
<i>Corynosoma obtusens</i>	<i>Halichoerus grypus</i>	New Zealand	JX442192	García-Varela <i>et al.</i> , 2013
<i>Corynosoma villosum</i>	<i>Callorhinus ursinus</i>	USA	MK119251	Lisitsyna <i>et al.</i> , 2019
<i>Corynosoma validum</i>	<i>Callorhinus ursinus</i>	USA	MK119252	Lisitsyna <i>et al.</i> , 2019
<i>Corynosoma enhydri</i>	<i>Enhydra lutris</i>	USA	DQ089719	García-Varela & Nadler, 2006
<i>Corynosoma magdaleni</i>	<i>Phoca vitulina</i>	Germany	MF078642	Waindok <i>et al.</i> , 2018
<i>Corynosoma nortmeri</i>	<i>Phoca vitulina</i>	Germany	MF001278	Waindok <i>et al.</i> , 2018
<i>Corynosoma strumosum</i>	<i>Phoca vitulina</i>	USA	EF467870	García-Varela & Pérez-Ponce de León, 2008
	<i>Pusa hispida botnica</i>	Finland	EF467871	García-Varela & Pérez-Ponce de León, 2008
<i>Bolbosoma balaenae</i>	<i>Zalophus californianus</i>	USA	MK119250	Lisitsyna <i>et al.</i> , 2019
	<i>Balaenoptera physalus</i>	Italy	MZ047281	Santoro <i>et al.</i> , 2021
<i>Bolbosoma turbinella</i>	<i>Eschrichtius robustus</i>	USA	JX442189	García-Varela <i>et al.</i> , 2013
<i>Andracantha phalacrocoracis</i>	<i>Zalophus californianus</i>	USA	MK119254	Lisitsyna <i>et al.</i> , 2019
<i>Hexaglandula corynosoma</i>	<i>Nyctanassa violacea</i>	Mexico	EU189488	Guillén-Hernández <i>et al.</i> , 2008
<i>Pseudocorynosoma anatarium</i>	<i>Bucephala albeola</i>	Mexico	KX688148	García-Varela <i>et al.</i> , 2017
<i>Pseudocorynosoma tepehuanesi</i>	<i>Oxyura jamaicensis</i>	Mexico	KX688139	García-Varela <i>et al.</i> , 2017
<i>Polymorphus obtusus</i>	<i>Aythya affinis</i>	Mexico	JX442195	García-Varela <i>et al.</i> , 2013
<i>Profilicollis bullocki</i>	<i>Emerita analoga</i>	Mexico	JX442197	García-Varela <i>et al.</i> , 2013
<i>Profilicollis chasmagnathi</i>	<i>Oligosarcus jenynsii</i>	Argentina	MT580124	Levy <i>et al.</i> , 2020
<i>Polymorphus trochus</i>	<i>Fulica americana</i>	Mexico	JX442196	García-Varela <i>et al.</i> , 2013

* – direct submission of unpublished data to GenBank



Figs. 15–20. SEM of spines in male and female specimens of *Corynosoma australe* from the intestines of *Zalophus californianus* in California. 15. Anterior trunk spines in the bulbous area. 16. Transition area between bulbous spines (right) and posterior trunk spines. 17–19. Continuous ventral spines in one female specimen: 17. Midventral spines. 18. Posterior ventral spines. Note that the field of spines anterior to the genital spines constricts (arrow) but remains continuous with the genital spines without breaks. 19. Another, more detailed, perspective of posterior ventral spines of the same female in Fig. 17, 18 with arrow pointing to greatest constriction. Female gonopore is on the opposite, ventral, side (dorso-subterminal). 20. Posterior end of a male specimen with invaginated bursa revealing the organization of the genital spines there.

smooth, without distinguishing markings or ornamentation (Fig. 31), with marked polar prolongation of fertilization membrane and 4 membranes (Fig. 32) with markedly lower level of metals than egg center.

Taxonomic summary

Type host. Australian sea lion (hair seal) *Neophoca cinerea* (Otariidae)

Additional host. California sea lion, *Zalophus californianus* (Otariidae).

Type locality. Pearson Island, South Australia

Current locality: The Pacific coast near San Francisco, California (37°46' N; 122°25' W).

Site of infection. Intestine (caecum, colon)

Specimens. HWML Helminthological Coll. No. 216825 (12 voucher specimens on 3 slides). Specimens from the South Australian Museum and the U.S. National Museum were not available; loans were banned since COVID times.

Representative DNA sequence. The 18S rDNA and mt Cox1 sequences of *Corynosoma australe* were deposited in GenBank under the accession numbers ON614192, ON614199 and ON619618, ON614719, respectively.

Remarks

Our subset of 29 specimens allowed us to give the first complete description of the California population of 1,201 specimens *C. australe* collected from 1 sea lion. Lisitsyna *et al.* (2019, Table 2) provided measurements of another set of 51 specimens from the same sea lion. These measurements, not repeated herein, did not distinguish between anterior vs. posterior testes (similar sizes) and included measurements of the blade and root of one hook (the largest); additional measurements and counts were not included. We added measurements of cement glands, bursa, neck, and three hooks (apical, middle and posterior), female reproductive system, and the number of genital spines, to our description. An account of our smaller subset of 10 males and 12 females from the same California collection was briefly outlined by Lisitsyna *et al.* (2018) and the fewer measurements provided there were similar to those reported by Lisitsyna *et al.* (2019).

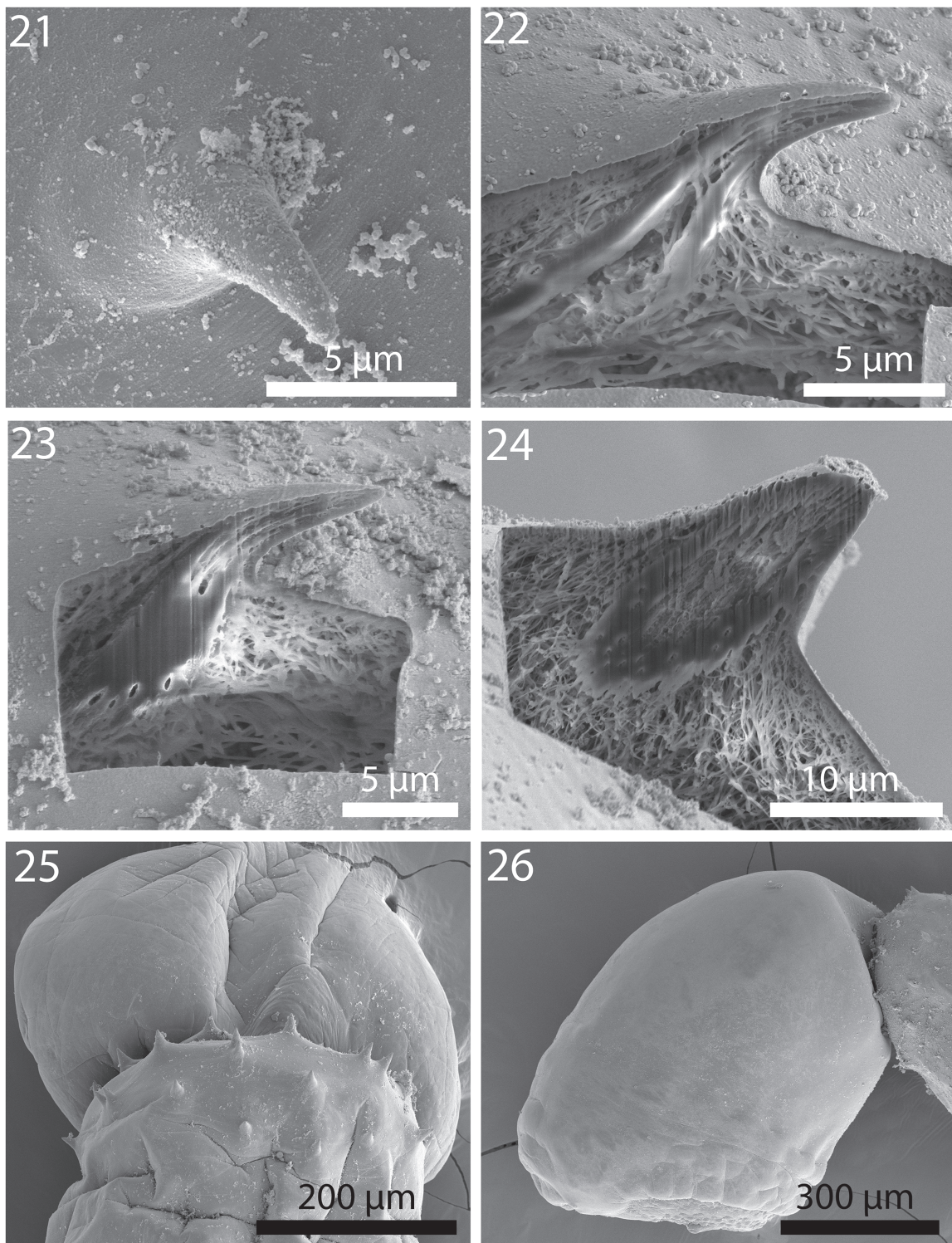
Smales (1986) redescribed *C. australe* from *Neophoca cinerea* (type host) and *Arctocephalus pusillatus* in South Australia with measurements comparable to but at variance with measurements of our California material from *Zalophus californianus*. All variations, and those among other collections compared in Tables 3, 4 of Lisitsyna *et al.* (2019), fell within the expected range of intraspecific variations. A number of differences, however, marred the redescription based only on the actual text since the Australian materials were not available on loan. For instance, Smales (1986), described the small posterior spine-like hooks as “last 4 to 5 hooks without roots” (p. 92), “the last one to four small without roots” (p. 95), and later in the Remarks section as “posterior three to four are smaller and rootless” (p. 95). The difference in the number of these hooks aside, these small posterior hooks are not rootless as shown in figure 9 of Smales (1986) (p. 93); they have prominent anterior roots (manubria) as observed by us and demonstrated by a few other observers, i.e., Zdzitowiecki (1984, Fig. 2B, p. 362). Zdzitowiecki (1984, Table I, p. 363) also provided measurements of 1 complete row of hook blades and roots in a male. Lisitsyna *et al.* (2018, p. 187) also noted the anterior roots of the small posterior spine-like hooks, and also described “1–2 hooks transitional with small roots in the shape of inverted Y (fig. 2E).” In her line drawing (Fig. 8, p. 93), Smales (1986) also showed a large space, between the anterior larger hooks and the posterior spine-like hooks, which was not observed. Among the large hooks, Smales (1986) stated “First 9 to 10 hooks have well-developed roots, as long as or longer than the hook” (p. 92) and in Fig. 9 depicts roots as long as blades anteriorly but considerably longer than blades posteriorly. We have, however, observed that the roots are markedly shorter than the blades of all hooks except the last two where they are of a comparable length; see Table I in Zdzitowiecki (1984).

After having reported 22 California specimens as *C. obtuscens* (Lisitsyna *et al.*, 2018), Lisitsyna *et al.* (2019) compared a similar subset of 51 specimens with those in 5 other collections reaching the conclusion that *C. australe* and *C. obtuscens* are the same species. This conclusion is novel and should be seen in the light of Johnston and Edmonds (1953) and Zdzitowiecki (1984) who have already noted the similarity of the two species before, and the history of the synonymy is listed in Gibson and Wayland (2022).

Table 4. Chemical composition of trunk spines and eggs of *Corynosoma australe* from *Zalophus californianus* in California.

Elements*	Spines (longitudinal sections)			Eggs (cross sections)	
	Anterior	Middle	Posterior	Edge (shell)	Center (acanthor)
Magnesium (Mg)	0.00	0.00	0.09	0.00	0.50
Sodium (Na)	0.00	0.00	0.00	0.00	0.00
Phosphorous (P)	1.39	0.00	1.16	0.91	7.73
Sulfur (S)	12.64	5.97	15.61	0	2.30
Calcium (Ca)	1.64	1.07	1.96	1.34	3.41

*Palladium (Pd) and gold (Au) were used to count the specimens and the gallium for the cross-cut of the hooks. These and other elements: carbon (C), oxygen (O), nitrogen (N) common in organic matter are omitted. Data is reported in weight (WT%).



Figs. 21–26. Detail of spines in specimens of *Corynosoma australe* from the intestines of *Zalophus californianus* in California using SEM and Gallium-cut sections. 21. SEM of an anterior trunk spine in the bulbus area. 22. A longitudinal Gallium-cut section of an anterior bulbus spine. Note the structure of the core element. 23. A longitudinal Gallium-cut section of a mid-trunk spine. 24. A longitudinal Gallium-cut section of a posterior spine. Note the structural differences between the outline and core of the spine types. 25. A dorso-terminal view of the posterior end of a male specimen showing the arrangement of the genital spines. Compare with Fig. 20. 26. A lateral view of a bursa showing its distal undulations and part of the genital spines (right).

Morphometric variability was primarily of intraspecific nature as the dimensions of the trunk, neck, proboscis, hooks, spines, receptacle, lemnisci, reproductive structures usually overlapped. The only distinguishing difference between the 2 species was the distribution of ventral trunk spines in females; being invariably discontinuous posteriorly in males. In their original description, the female ventral spines were discontinuous posteriorly in *C. australe* but continuous throughout the total ventral aspect of *C. obtuscens*. The taxonomic history listed in Table 1 demonstrates this distinction in a few accounts but also demonstrates the opposite to various degrees in a few more accounts; see for instance Zdzitowiecki (1984), Sardella *et al.* (2005) and Hernández-Orts *et al.* (2017a). Lisitsyna *et al.* (2019) also found a small spine-free zone in an allotype of *C. obtuscens*, among other overlaps and inconsistencies, and “confirmed the variability in the arrangement of somatic spines on the ventral surface of the body of females.” The constriction of the field of posterior ventral spines in our specimens (Figs. 18, 19) offers a plausible resolution for the controversy of the presence or absence of posterior ventral spines in females. We propose that spines on this part of the female ventral trunk are labile and may constrict to the extreme point of total absence and separation of the two spine fields, or not at all.

There are also additional issues with spines. Zdzitowiecki (1984) reported 11 – 28 and 20 – 40 genital spines in males and females, respectively. We found considerably more genital spines in males than in females. Zdzitowiecki (1984) also correctly mentioned that the male genital opening is terminal while Lisitsyna *et al.* (2018) reported a subterminal opening in both sexes and Johnston (1937) reported a terminal opening in females; both are not in agreement with our observations.

Our microscopic study revealed most unique anatomy of the female reproductive system first observed among the thousands of specimens of many acanthocephalan species that we have examined. We noted in two clear specimens that were not congested with eggs a reproductive system making up 70 % of worm length with normal vaginal sphincters, uterine bell and a very long uterus with the uterine bell cells (SA) in the mid-point of the long uterus and not at the base of the uterine bell where it is commonly found in other species of acanthocephalans. This unique position of the

SA away from the uterine bell where they normally function in direct coordination with the uterine bell is of great diagnostic value that represents a functional enigma. No reference was made to the complete female reproductive system in the descriptions of Johnston (1937) or Lincicome (1943) or any other taxonomic accounts except for an occasional line drawing of the vagina and posterior female trunk tip as in Zdzitowiecki (1984, Fig. 2d, p. 362). However, Zdzitowiecki’s (1984) Fig. 2e of a “uterine bell” was incomplete; showing a questionable position of a 4-nucleated selective apparatus cells overlapping its base and appeared to be at the distal end of the reproductive system. In reality, the glands are multicellular and are found in the middle of the uterus and not at its anterior end as characteristically peculiar in this species. The operational aspects of the selective apparatus need to be revised in light of this finding. In her redescription of *C. australe*, Smales (1986, Fig. 10, p. 93) drew an outline of a small female reproductive system with barely visible uterine bell and vagina showing no selective apparatus glands anywhere, within a female body; without an accompanying text. Only Zdzitowiecki (1984, p. 363) stated that “Total length of the (female) genital system, from the anterior margin of the uterine bell to the genital opening is equal to 1.1 – 1.4 (mm)” in his Antarctic specimens is comparable to our measurements of the posterior half of the genital system up to the selective apparatus pouches which Zdzitowiecki (1984) apparently interpreted as the uterine bell and created a figure (Fig. 2e, p. 362) for it. He clearly did not see the anterior half of the reproductive system ending up with the real uterine bell perhaps because of the usual congestion of the body cavity with eggs which has been the case in almost all our other specimens.

Micropores

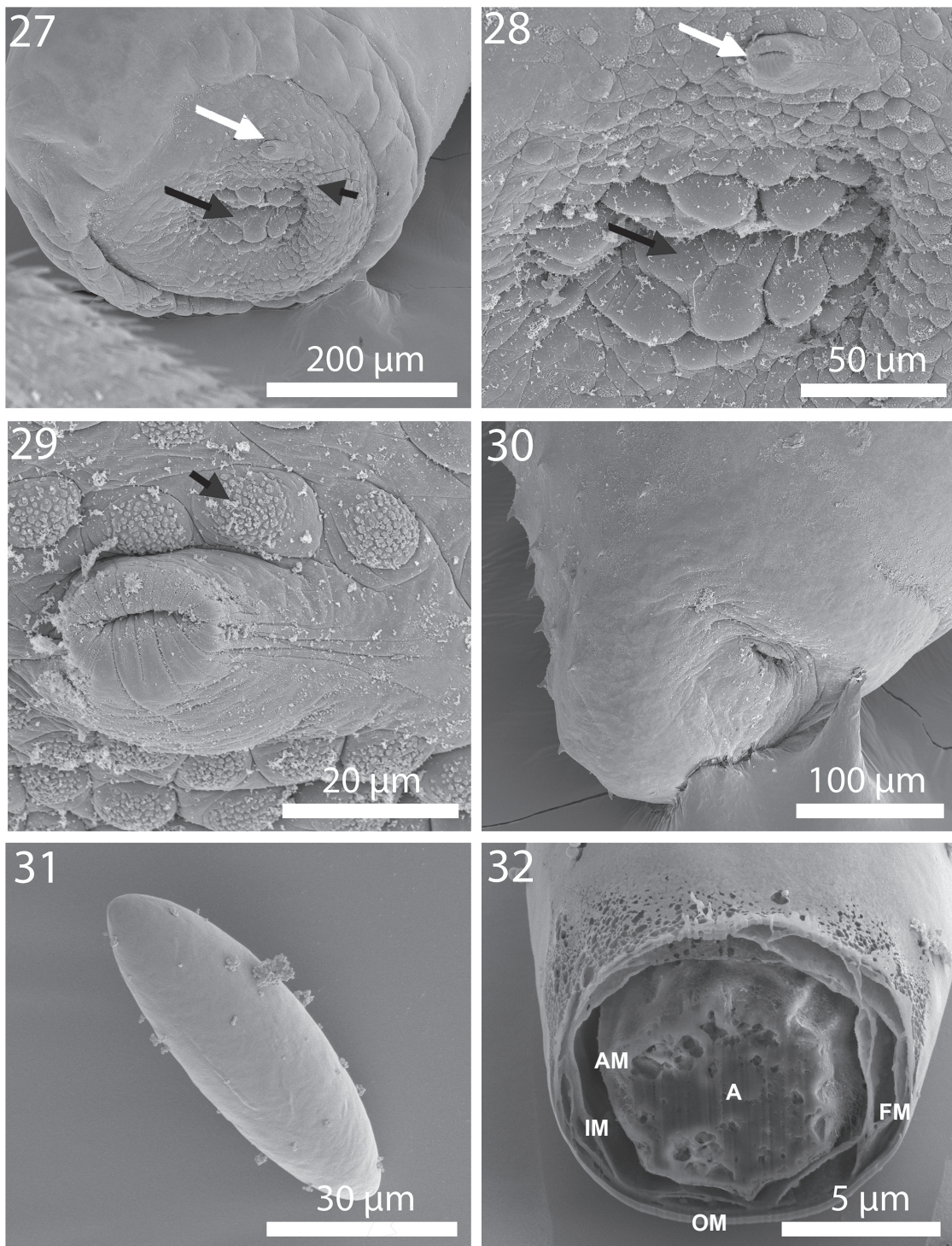
The trunk and other structures including the proboscis, proboscis hooks, and spines (Figs. 10 – 14) had apparent osmiophilic micropores of various diameters, shapes and distribution in various body parts. In this small acanthocephalan, every possible external surface is studded with micropores. In some areas, the micropores were more widely spaced compared to the usual more widely distributed micropores more often observed in other acanthocephalan species.

Table 5. Chemical composition and localization of elements in hooks of *Corynosoma australe* from *Zalophus californianus* in California.

Element*	Anterior hooks			Middle hooks				Posterior hooks	
	Tip x-section	Middle	Longitudinal section	Tip x-section	Tip edge	Middle x-section	Middle edge	Tip x-section	Middle edge
Magnesium (Mg)	1.21	0.23–1.67**	0.02–0.07	0.63	0.62	1.61	0.66	0.02	0.78–1.52
Sodium (Na)	0.25	0.00–0.04	0.00–0.03	0.00	0.03	0.08	0.00	0.02	0.05–0.07
Phosphorous (P)	9.95	15.74–18.71	12.78–20.35	10.64	11.00	21.32	16.10	2.82	14.91–20.49
Sulfur (S)	2.96	0.09–7.10	0.34–3.50	5.50	15.38	0.03	4.34	23.52	1.18–14.09
Calcium (Ca)	18.99	30.80–34.84	32.03–72.06	19.98	19.11	42.48	34.18	3.16	27.05–40.39

*Palladium (Pd) and gold (Au) were used to count the specimens and the gallium for the cross-cut of the hooks. These and other elements (carbon (C), oxygen (O), nitrogen (N)) common in organic matter are omitted. Data is reported in weight (WT%). Bolded numbers are represented in Figs. 25–27.

** A range indicates that 3 hooks were analyzed.



Figs. 27–32. External orifices of male and female reproductive systems and eggs of *Corynosoma australe* from the intestines of *Zalophus californianus* in California using SEM and Gallium-cut sections. 27–29. The male bursa. 27. Bursa with the undulating lip, penis (white arrows), central cluster of prominent sensory bulbs (black arrows), and surrounding circles of specialized sensory domes (short black arrows). 28. The central part of a bursa showing the two types of sensory structures and the penis. 29. A higher magnification of the penis and the surrounding type of sensory domes. 30. The posterior end of a female showing the dorsal gonopore (right) and the continuity of the posterior ventral spines with the genital spines. 31. A smooth egg with no external ornamentation or dentations. 32. A cross Gallium-cut section of an egg showing 3 external egg shell membranes FM: fertilization membrane, IM: inner membrane, OM: outer membrane) with the fourth tightly enveloping the acanthor (A).

Energy Dispersive x-ray analysis (EDXA)

The relative WT% concentrations obtained by the TEAM software for hooks, spines, and eggs of *C. australe* from a California sea lion, *Z. californianus* in California are reported in Tables 4 – 5 and Figs. 37 – 39. Our EDXA results of *C. australe* show a center core with a high level of sulfur at the tip of the middle and posterior hook's edge (15.38 %) and cross-section (23.52 %), respectively, but considerably lower (2.96 %) at the tip of anterior hooks. The EDXA spectra of cross sections of the middle of all hooks showed extremely high concentrations of Calcium and Phosphorus characteristic of the center core of hooks. The presence of Sulfur, Calcium, and Phosphorus in the EDXA spectra obtained from the edge of the hook base cross-section is attributed to the proximity of the exterior shell to the center core. In anterior and posterior spines, the sulfur level was highest, 12.64 and 15.61, respectively, but markedly lower in the weak middle spines at 5.97 % (Table 4) while the levels of phosphorus and calcium were minimal. The egg center had a higher level of metals especially phosphorous (7.73 %) compared to the egg shell (0.91 %) (Table 4). It is worth noting that, these reported WT% numbers should not be inter-

preted as compositional. They are, however, indicative of general compositional differences observed between the selected areas.

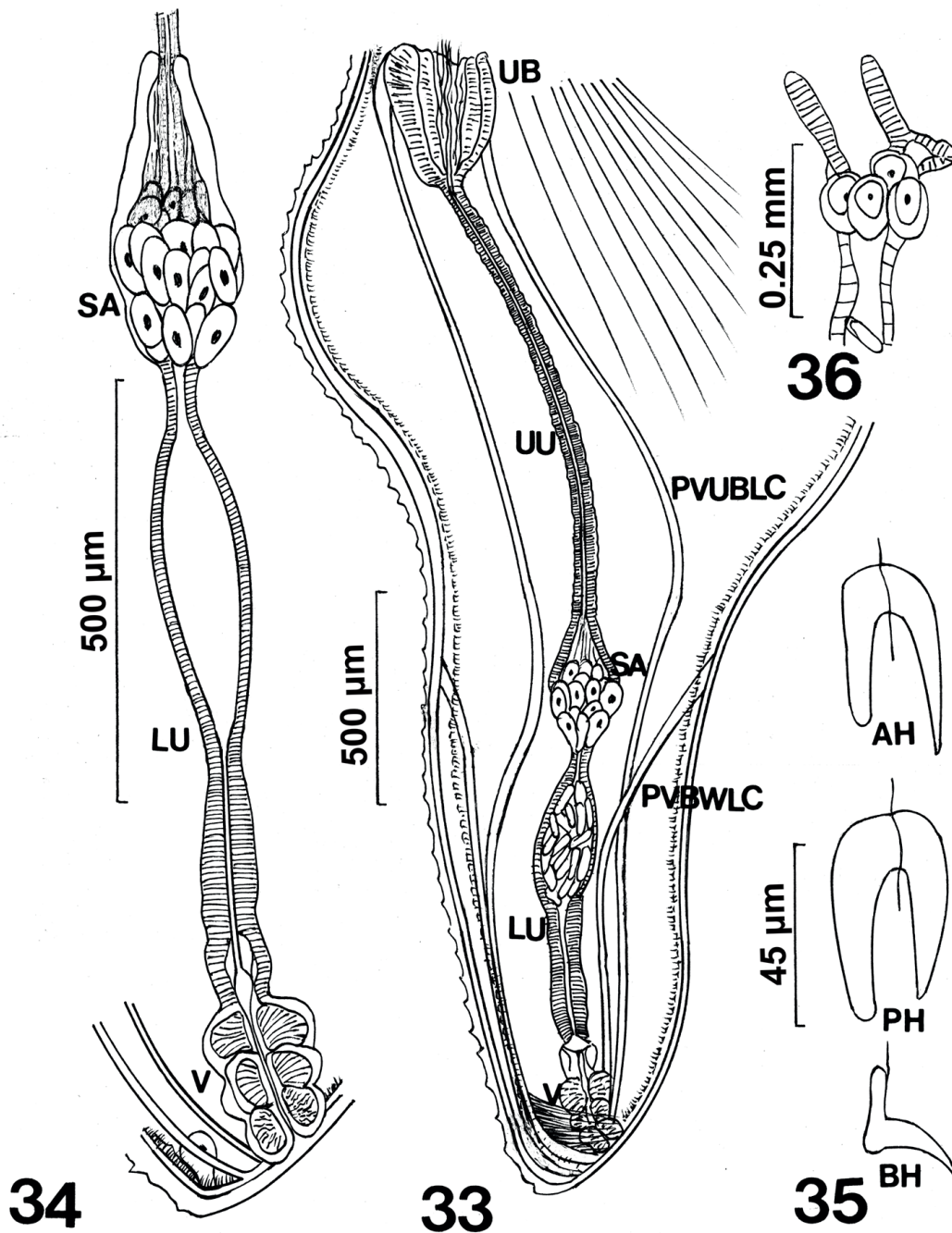
Molecular results

In the present study, a total of four partial 18S and Cox1 sequences of *C. australe* were generated. On the GenBank database, most of the sequences available for *C. australe* are of mt gene Cox1 and only two sequences are of 18S gene. So, for a better comparative phylogeny and to provide information related to the population relationship of *C. australe* we have provided a detailed analysis of Cox1 gene along with 18S gene analysis. Newly generated 18S sequences of *C. australe* were almost identical, shows 0.02 % genetic divergence. The sequence for *C. australe* from USA (MK119255) infecting the same host *Z. californianus* exhibited genetic divergence was 0.27 %, while with another isolate from Mexico (JX442168) infected *Phocartos hookeri* divergence was 1.5 %. The phylogenetic analyses inferred with maximum likelihood (ML) and Bayesian inference (BI) methods yielded similar topologies (Fig. 40). In both phylogenetic trees, *C. australe* was placed with the other isolates of similar species in a clade having

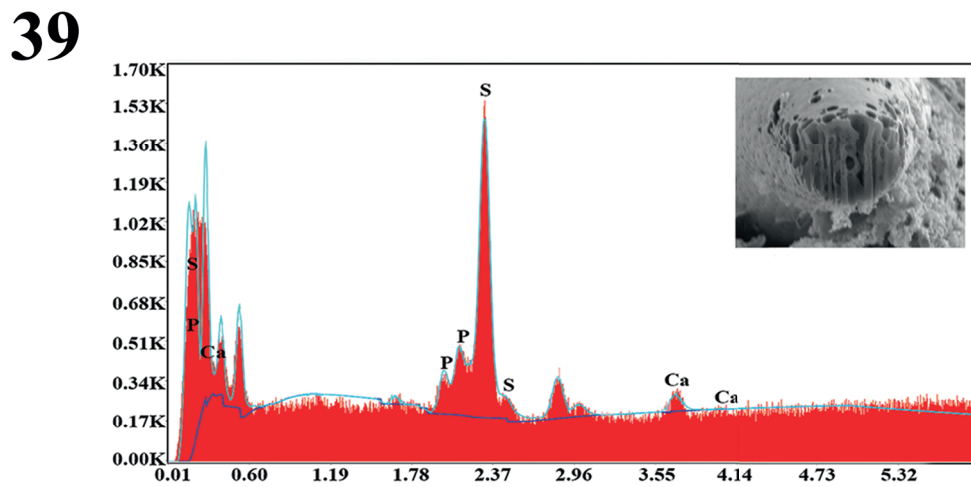
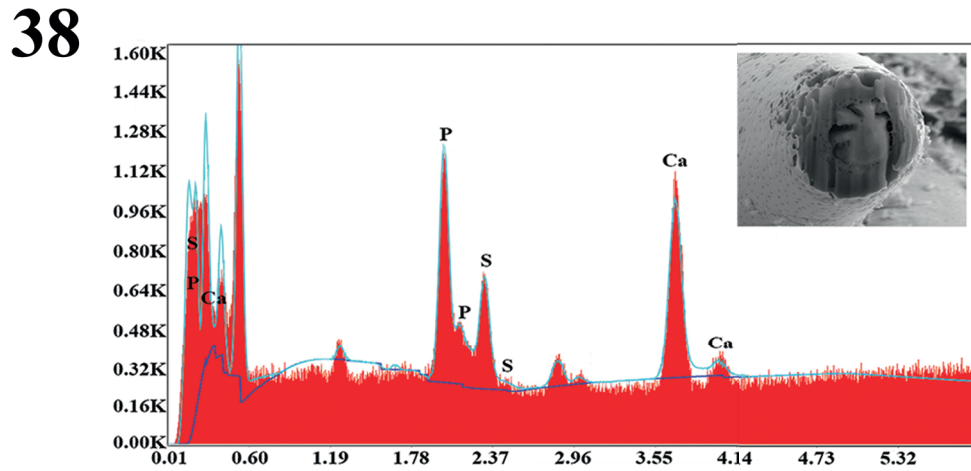
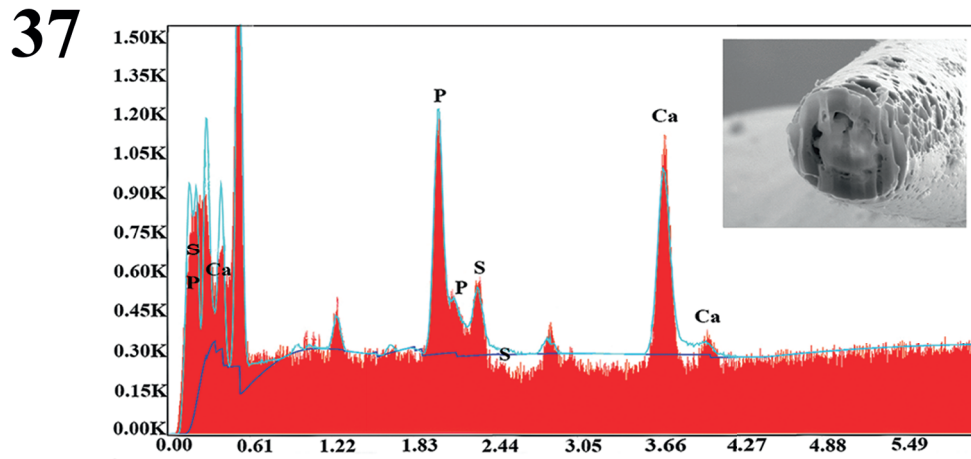
Table 6. Data for the population of *Corynosoma australe* used in the haplotype networking using mt Cox1 gene. Asterisk shows sequences unpublished on NCBI database. Newly generated sequences are presented in bold.

Geographical Locality*	Cox1 Haplotype no.	ID in Fig. 46	GenBank accession nos.	References
Pacific coast near San Francisco, California, USA	H1	U1	ON619618, ON614719	Present study
Sausalito, California, USA	H2	U	MK119245-MK119249	Lisitsyna <i>et al.</i> 2019
Baja California, Mexico	H2	M	MT676816-MT676818	García-Varela <i>et al.</i> 2021
Rio de Janeiro, Brazil	H3	B	KU314822	Fonseca <i>et al.</i> 2019
Chubut, Argentina	H4	A	MW724483	Hernández-Orts <i>et al.</i> 2021
Baja California, Mexico	H5	M	MT676813	García-Varela <i>et al.</i> 2021
Sonora, Mexico	H6	M	MT676811	García-Varela <i>et al.</i> 2021
Baja California, Mexico	H7	M	MT676814	García-Varela <i>et al.</i> 2021
Sonora, Mexico	H8	M	MT676810	García-Varela <i>et al.</i> 2021
Northern Patagonia, Argentina	H9	A	MT676821	García-Varela <i>et al.</i> 2021
Sonora, Mexico	H10	M	MT676809	García-Varela <i>et al.</i> 2021
Baja California Sur, Mexico	H11	M	MT676808	García-Varela <i>et al.</i> 2021
Northern Patagonia, Argentina	H12	A	MT676823	García-Varela <i>et al.</i> 2021
Northern Patagonia, Argentina	H13	A	MT676819, MT676820, MT676822	García-Varela <i>et al.</i> 2021
Baja California, Mexico	H14	M	MT676815	García-Varela <i>et al.</i> 2021
Northern Patagonia, Argentina	H15	A	MT676824	García-Varela <i>et al.</i> 2021
Northern Patagonia, Argentina	H16	A	MF497333	Hernández-Orts <i>et al.</i> 2021
Baja California, Mexico	H17	M	MT676812	García-Varela <i>et al.</i> 2021
Rio de Janeiro, Brazil	H18	B	MF497335	Hernández-Orts <i>et al.</i> 2021
Northern Patagonia, Argentina	H19	A	MF497334	Hernández-Orts <i>et al.</i> 2021
Northern Patagonia, Argentina	H20	A	KX957714	Fonseca <i>et al.</i> 2019
Peru	H21	P	MZ920052, MZ920053, MZ920055, MZ920056-MZ920062, MZ920064-MZ920067	Mondragon-Martinez <i>et al.</i> 2021*
Peru	H22	P	MZ920054, MZ920063	Mondragon-Martinez <i>et al.</i> 2021*

*Abbreviations used for isolates country: U1 – present study isolates from USA, U – USA, M – Mexico, B – Brazil, A – Argentina, P – Peru.



Figs. 33–36. Line drawings of the female reproductive system and 3 selected hooks of *Corynosoma australe* from the intestines of *Zalophus californianus* in California. Fig. 33. The whole reproductive system of a 3.2 mm. long female. Note the presence of the Selective apparatus (SA) almost half way between the upper uterus (UU) connecting with the uterine bell (UB) and the lower uterus (LU) connecting with the dorsal vagina (V). Also note the dorsal and ventral short paravaginal ligament cords inserting in the body wall (PVBWLC) and the dorsal and ventral longer paravaginal ligament cords connecting with the uterine bell (PVUBLC). The para-vaginal muscular sheet wrapping around vagina can be observed. The continuity of trunk spines on the ventral side is evident. Fig. 34. A higher magnification of the posterior half of the reproductive system of a second female. Posterior muscular wrap not shown. Fig. 35. The 3 hook types: an anterior slender subapical hook (AH) with shorter root; a robust hook at the inflated part of the posterior proboscis (PH) with slightly longer root; and a small curved basal or near-basal hook (BH) with anteriorly directed root (manubrium). Fig. 36. The "uterine bell" of *Corynosoma australe* after Zdzitowiecki (1984, Fig. 2e, p. 362).



Figs. 37–39. Energy Dispersive X-Ray spectra of Gallium cut anterior hook tip x-section (37), middle hook tip x-section (38), and posterior hook tip x-section (39) showing levels of sulfur in calcium and phosphorous in all hooks See Table 2 for more specific figures (bolded). Insets: SEM of Gallium cut anterior hook tip cross-section (37), SEM of Gallium cut middle hook tip cross-section (38), and SEM of Gallium cut posterior hook tip cross-section (39). Note the high levels of calcium and phosphorous in anterior and middle hooks and the high level of sulfur in posterior hooks.

strong bootstrap and Bayesian probability values (Fig. 40). In the newly generated Cox1 sequences of *C. australe* shows only 0.04 % intraspecific genetic divergences. Our phylogenetic tree showed that the genus *Corynosoma* is comprised of two main subclades – the first one A comprises specimens of *C. australe* from different regions in North America, i.e., the USA and Mexico, and the second one B comprises Brazil, Argentina and Peru in South America available in the GenBank database. All isolates of subclades A and B were nested in a monophyletic clade as they are the same species (Fig. 41). In the present study, Cox1 sequences of *C. australe* showed a strong relationship with sequences of Lisitsyna *et al.* (2019) from California, USA (genetic divergence was 0.9 %). The phylogenetic analyses deduced with ML and BI methods produced the same topologies. Both trees placed the specimens of *C. australe* in a clade obtaining strong bootstrap support and Bayesian posterior probability values (Fig. 41). The genetic divergence between the present isolates and those available in GenBank from

different regions ranged from 0.9 to 3.0 %. The sequence for *C. australe* suggests that in comparison with other isolates of *C. australe* it exhibited the lowest divergence level with the isolates from the USA and the highest divergence level with the isolates from Peru (3.0 %). We also agreed with Hernández-Orts *et al.* (2017b) that *C. hanna* is a sister taxon to *C. australe* as both species shares close clades (Fig. 41). Another clade comprises species as different lineages as *C. semerme* together with *C. obtuscens*, *C. villosum* plus the sequence of *C. validum*, *C. enhydri* along with *C. magdalen* isolates and a separate lineage was formed by the sequences identified as *Corynosoma strumosum* (Fig. 41). Lisitsyna *et al.*, 2019 mentioned in their study that the morphological study of the isolates in the publication of García-Varela *et al.* (2013) was not possible due to the lack of specimens and that the species was misidentified. They also made it clear in their study that the cox1 sequence (JX442192) (Fig. 41) as well as the 18S rDNA sequence (JX442169) (Fig. 40) of *C. obtuscens* published by García-Varela

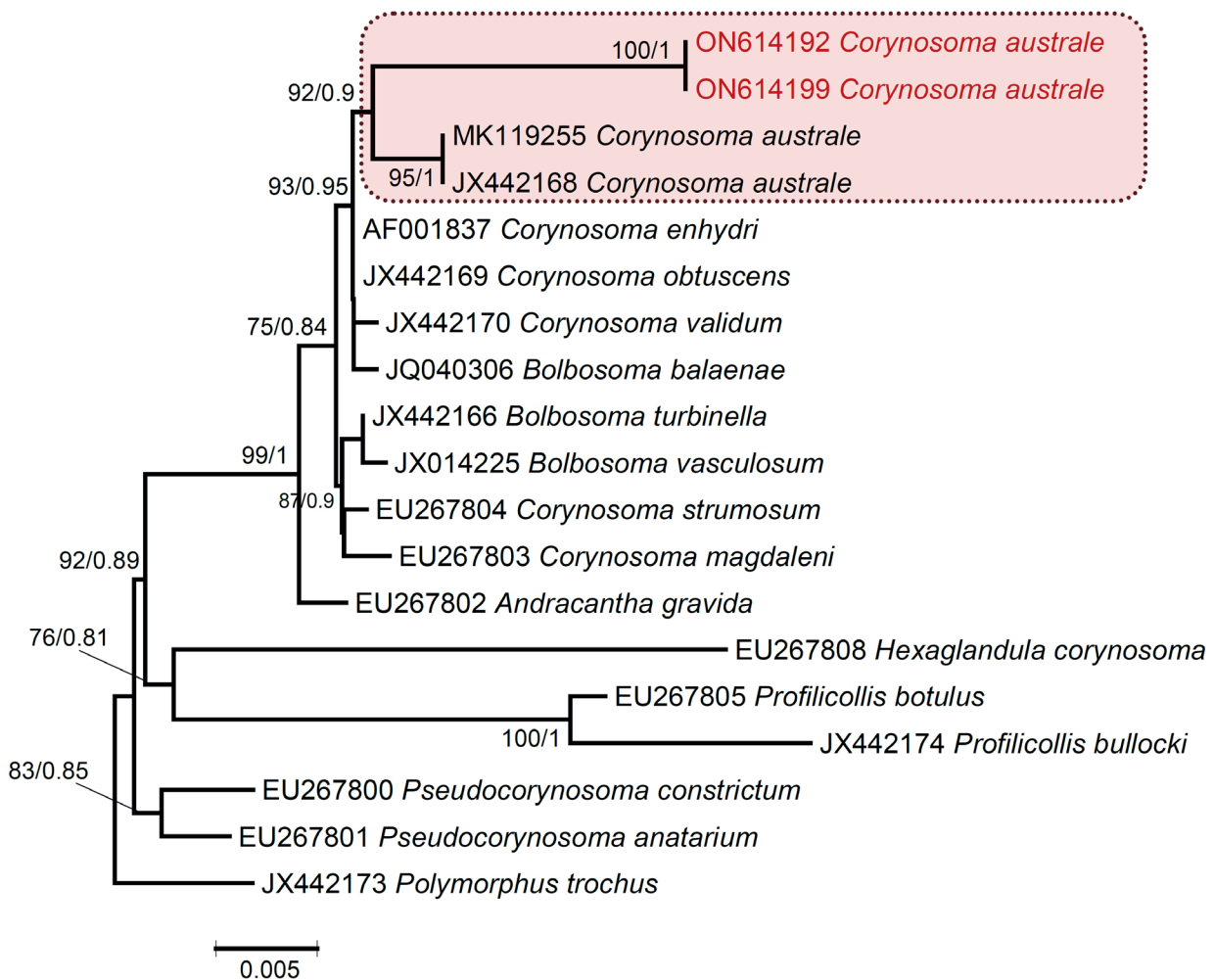


Fig. 40. Phylogenetic relationships inferred using 18S gene sequences of *Corynosoma australe* and other acanthocephalan species. Nodal support from the two analyses is indicated as ML/BI and indicates values of bootstrap >70%. The scale-bar indicates the expected number of substitutions per site.

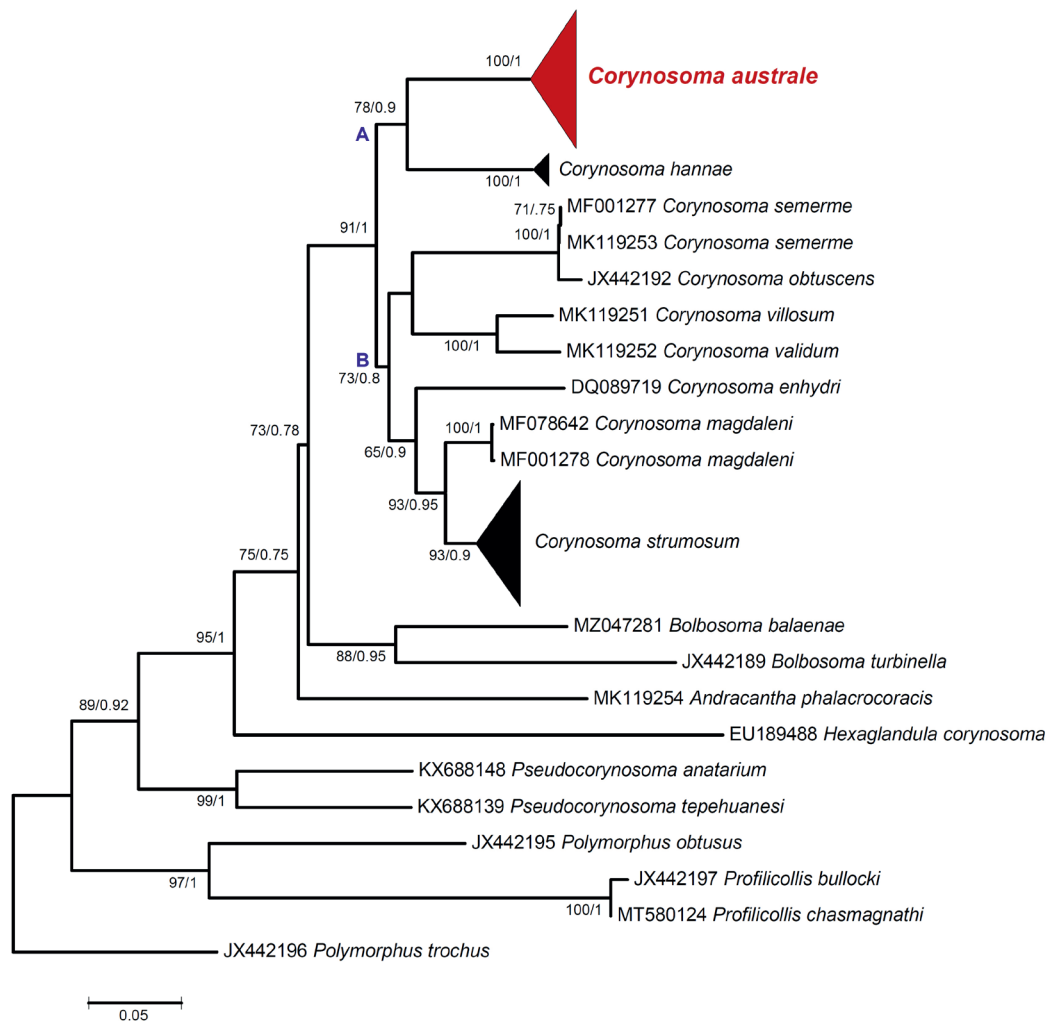


Fig. 41. Phylogenetic reconstruction using mt Cox1 sequences of *Corynosoma australe* and sequences of other Acanthocephala deposited in the GenBank. The numbers indicate values of bootstrap >50%. Numbers above branches indicate nodal support as maximum likelihood (ML) and posterior probabilities from BI. The scale-bar indicates the expected number of substitutions per site.

et al. (2013) show *C. semerme* instead of *C. obtuscens*. In our study, a haplotype network was constructed inferred with 46 specimens of *C. australe* as shown in Fig. 42. In the complete analysis, 22 haplotypes were detected (Table 3). The H1 haplotype (H1, $n = 2$) are the specimens collected in the present study from the Pacific coast near San Francisco, California corresponded to specimens from North America. H2 Haplotype (H2, $n = 8$) are shared by *C. australe* populations from Mexico and Sausalito, California, the USA (approximately 10 miles north of San Francisco from where we have collected our specimens). Haplotypes H3 and H4 were found in Brazil and Argentina, respectively corresponding to the population of *C. australe* from South America. Haplotypes H5–H8 and H10, H11, H14, and H17 were found in Mexico corresponding to the specimens from North America. Haplotypes H9, H12, H13, H15, H16 and H20 were reported as *C. australe* populations of

Argentina. Haplotypes H18 and H19 were found from Brazil and corresponded to specimens from South America. Furthest haplotype (H21, $n=14$) and haplotype H22 were found off the Peruvian coasts (Fig. 42). A separate tree was also constructed in the present analysis for the isolates of *C. australe* representing clusters as in congruence of the haplotype network (Fig. 43). Additionally, isolates collected in the present study fell within a strongly supported clade representing the North American isolates of *C. australe* (Fig. 43).

Discussion

Morphological findings

Our report provides new insights on the morphology of structures not previously reported in the many descriptive accounts

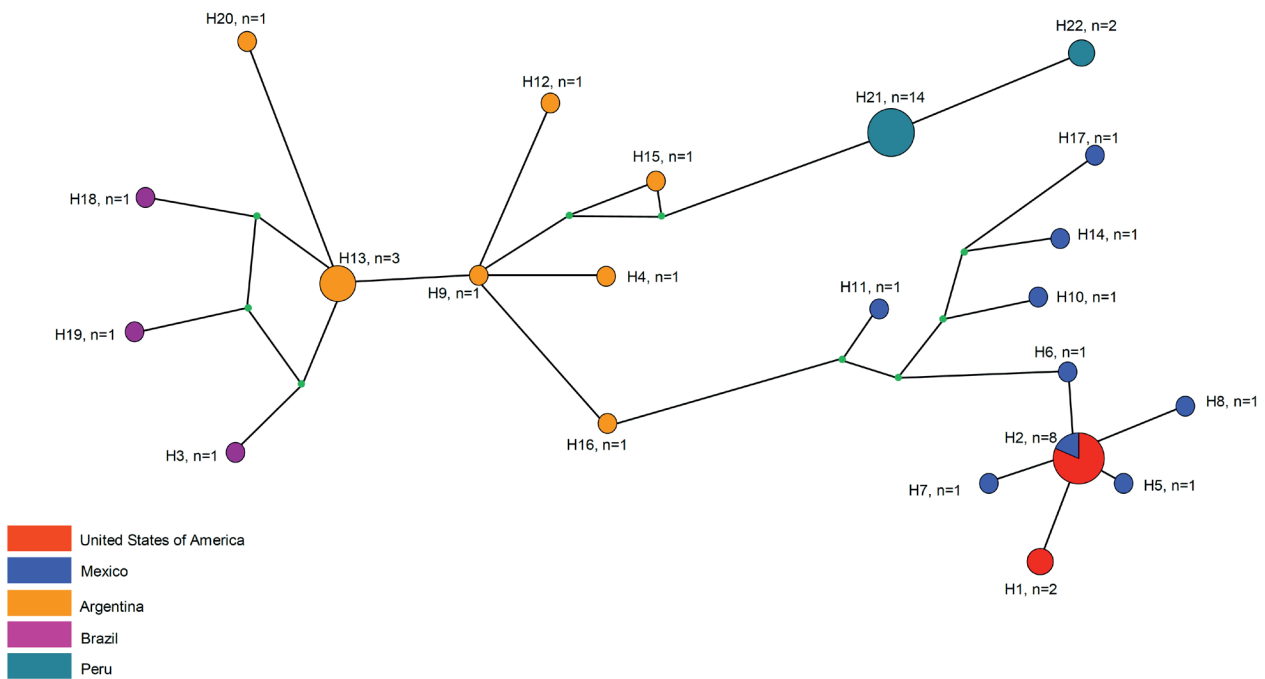


Fig. 42. Median-joining haplotype networks based on Cox1 sequence data of *Corynosoma australe*. Each circle size represents the frequency of a haplotype as in the population.

of *C. australe* against the backdrop of works by other observers summarized in Table 1. We explore these new insights in the following points.

1. The controversy of the identity of *C. australe* vs. that of its synonym *C. obtuscens* boiled down to differences in the distribution of ventral trunk spines in females, being continuous in *C. obtuscens* and disjunct in *C. australe*. A summary of these controversies is presented in Table 1 which shows that this character is variable but no plausible explanation was provided to explain this variability. We provided evidence of variable constriction in the posterior field of ventral spines (Figs. 18, 19) that when extremely restricted will produce a separation in the more anterior and posterior fields. In our specimens, the ventral trunk spines were invariably continuous but the degree of posterior constriction varied.

2. The anatomy of the female reproductive system was invariably incompletely reported. In almost all reports, only the posterior-most part showing the vagina and posterior-most extremity of the uterus could be seen; for example, see Smales (1986) and Zdzitowiecki (1984, 1991). Only Zdzitowiecki (1984) measured the posterior part of the reproductive system interpreting it as the whole system; the true uterine bell must have been obscured by eggs. He considered the SA as the uterine bell (see his Fig. 2e, p. 362 copied as our Fig. 36). The confusion is readily understandable as these acanthocephalan females are usually congested with eggs that almost invariably occupy the anterior inflated part of the trunk obscuring the anterior part of the reproductive system. We have provided the first description of the complete reproductive

system and identified the SA for the first time almost in the middle of the long uterus (Figs. 33, 34) and not at the base of the terminal anterior uterine bell where it has been invariably reported by other observers to date until our present finding. We have also provided the first description of four para-vaginal ligament cords; two short ones connecting to the body wall dorsally and ventrally, and two longer ones connecting to the uterine bell more anteriorly.

3. We have identified micropores on all body surfaces (Figs. 10 – 14) in an apparent adaptation to utilize as much body surface as possible for the process of nutrient absorption accommodating the small size of this acanthocephalan.

4. We provide considerable detail on the organization of the male reproductive system and show for the first time the elaborate sensory system of the bursa necessary for the successful completion of the copulatory process in *C. australe*. The shape and complexity of bursal sensory structures are species-specific but have rarely been reported by other observers. Halajian *et al.* (2020, p. 128) made a brief reference to “Bursal papillae surrounding the genital opening (their Figs. 9, 10) are noted” and Hernández-Orts *et al.* (2017a, Fig. 4 D, p. 9) showed an SEM of the genital spines on the posterior end of a male trunk. For a detailed SEM study of these sensory structures in the male reproductive organs of 28 species in 10 families and 5 orders of acanthocephalans, see Amin *et al.* (2020a).

5. We discuss trunk spines in new detail. Their distribution on all trunk surfaces (Figs. 1, 2), their ventral presence anterior to the usually reported anterior rings only (first report: Fig. 3, white

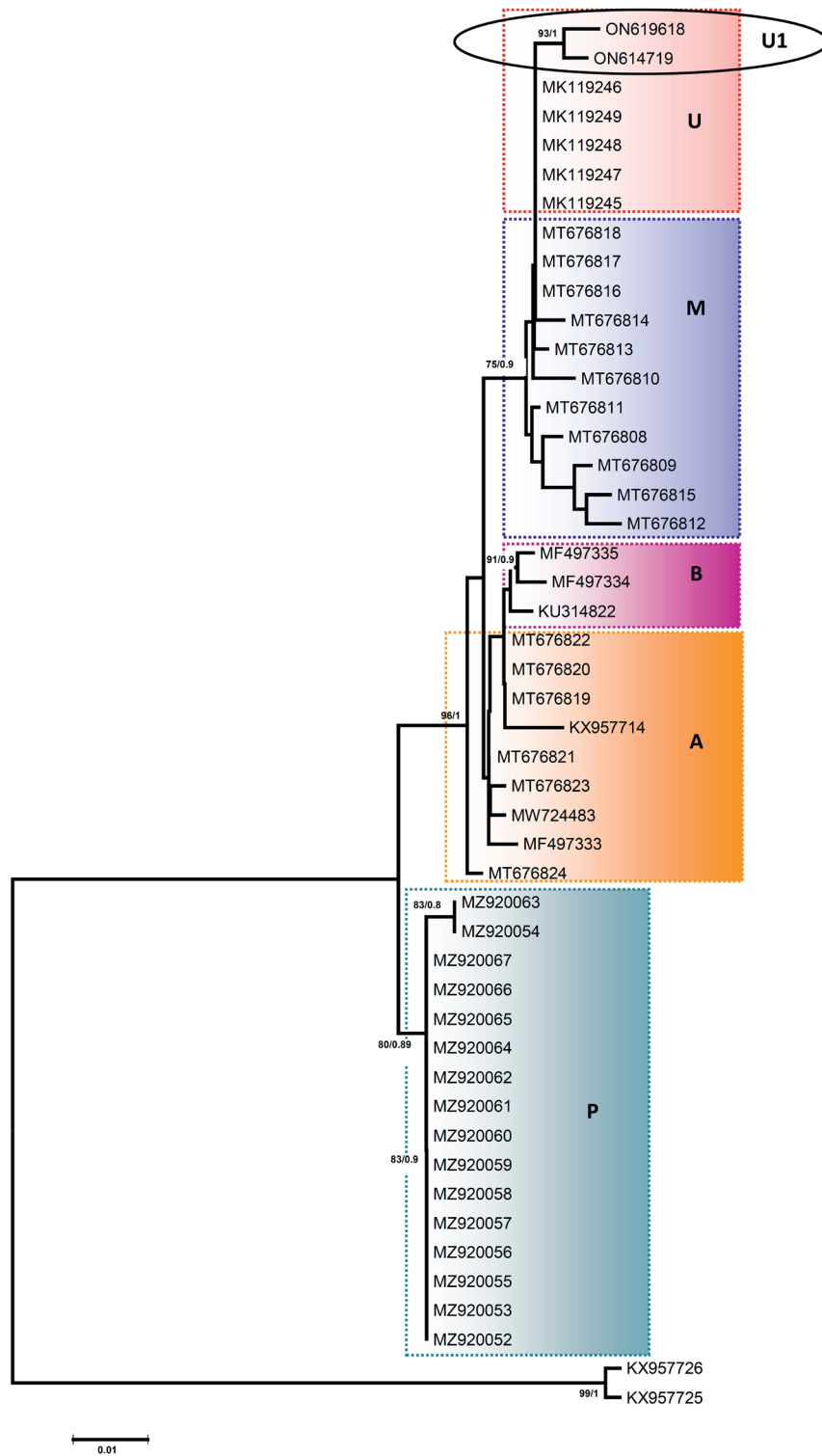


Fig. 43. Phylogenetic tree from Maximum likelihood and Bayesian inference analysis of the Cox1 sequences of *Corynosoma australe* population. Outgroup: *Corynosoma hanna*. The scale-bar indicates the expected number of substitutions per site. Abbreviations used for isolates country: U1- present study isolates from USA, U- USA, M- Mexico, B- Brazil, A- Argentina, P- Peru. The color refers to isolates obtained as in the haplotype network (Fig. 42; red: USA, blue: Mexico, orange: Argentina, magenta: Brazil, aqua blue: Peru).

arrow), the scanty and weak transitional spines (Fig. 16, arrow) with the lowest level of sulfur (Table 4) (first report) and comparative anatomy of anterior, transitional, and posterior spines (Figs. 22 – 24) (first report).

6. We provide EDXA of anterior, middle and posterior hooks and eggs for the first time (Tables 2, 3, Figs. 37 – 39) that clearly varied from that of another *C. australe* population studied from the Cape fur seal, *A. pusillus pusillus* in South Africa.

7. We provide SEM images suggesting the presence of an apical organ (Figs. 4, 5) and the anteriorly directed roots (manubrial) of the posterior-most spine-like hooks (Fig. 35). These hooks have been usually described as rootless spines/hooks; see the re-description by Smales (1986). The only other related reports are those of Lisitsyna *et al.* (2018, p. 187) who described them as “simple roots directed anteriorly or without roots” and Zdzitowiecki (1984) who included his Fig. 2b (p. 362) showing a lateral view of 1 hook row with the posterior-most hooks having anteriorly directed roots without a corresponding text reference.

Micropores

The micropores of *C. australe*, like those reported from other species of the Acanthocephala, are associated with internal crypts and vary in diameter and distribution in different trunk regions corresponding with differential absorption of nutrients. In *C. australe*, the micropores were distributed in most body surfaces that we have observed including the proboscis, proboscis’ hooks, trunk, and trunk spines as though to maximize the absorptive function of all surfaces of their small body. We have reported micropores in a large number of acanthocephalan species (Heckmann *et al.*, 2013) and in a few more since, and demonstrated the tunnelling from the cuticular surface into the internal crypts by TEM. Amin *et al.* (2009) gave a summary of the structural-functional relationship of the micropores in various acanthocephalan species including *Rhadinorhynchus ornatus* Van Cleave, 1918, *Polymorphus minutus* (Goeze, 1782) Lühe, 1911, *Monilliformis monilliformis* (Bremser, 1811) Travassos, 1915, *Macracanthorhynchus hirudinaceus* (Pallas, 1781) Travassos 1917, and *Sclerocollum rubrimaris* Schmidt and Paperna, 1978. Wright and Lumsden (1969) and Byram and Fisher (1973) reported that the peripheral canals of the micropores are continuous with canalicular crypts. These crypts appear to “constitute a huge increase in external surface area. implicated in nutrient up take.” Whitfield (1979) estimated a 44-fold increase at a surface density of 15 invaginations per 1 μm^2 of *M. monilliformis* tegumental surface. The micropores and the peripheral canal connections to the canaliculi of the inner layer of the tegument were demonstrated by transmission electron micrographs in *Corynosoma strumosum* (Rudolphi, 1802) Lühe, 1904 from the Caspian seal *Pusa caspica* (Gmelin, 1788) in the Caspian Sea (Figs. 19, 20 of Amin *et al.*, 2011) and in *Neoechinorhynchus personatus* Tkach, Sarabeev, Shvetsova, 2014 from flathead grey mullet *Mugil cephalus* Linn. 1758 in Tunisia (Figs. 26, 29, 30 in Amin *et al.*, 2020a).

Energy Dispersive X-ray Analysis (EDXA)

Our studies of acanthocephalan worms have usually involved EDXA of FIB-sectioned hooks and spines (Heckmann, 2006, Heckmann *et al.*, 2007, 2012; Standing & Heckmann, 2014). Our results of chemical ions of hooks, spines, and eggs of *C. australe* from the California sea lion, *Z. californianus* in California varied from those obtained by Halajian *et al.* (2020, Table 1, p. 129) for a different population of the same species, *C. australe*, from the Cape fur seal *Arctocephalus pusillus pusillus* off the Namibian coast, South Africa. In specimens from South Africa, one hook had markedly lower levels of Calcium (36.10 – 43.2 %) and of Sulfur (0.2 – 0.38) (Halajian *et al.*, 2020) compared to our specimens with 32.03 – 72.06 % and 0.34 – 3.50 % Calcium, respectively reaching 23.52 % Calcium at the tip of posterior hooks (Table 5), and spines had higher levels of Sulfur of 15.35 – 29.87 % than in our California specimens with 5.97 – 15.61 % (Table 4), among differences in other elements. The eggshell of the Namibian specimens also had considerably higher levels of Sulfur and Phosphorous. Such differences are probably related to parasite population variations, host species, and geography.

Sulfur is usually seen at the outer edge of large hooks and Calcium and Phosphorus are major ions in the base and middle of hooks where tension and strength are paramount for hook function. The following results of the EDXA of the FIB-sectioned hooks (dual beam SEM) are limited to those from our California *C. australe* material. The edge of the hook tips and the tip x-section of *C. australe* showed the highest level of Sulfur (15.38, 23.52). Comparable or higher levels of Sulfur were observed in other species of acanthocephalans. For instance, *Cavisoma magnum* (Southwell, 1927) Van Cleave, 1931 from *Mugil cephalus* in the Arabian Sea, has a similar pattern but considerably higher levels of sulfur in hook tips (43.51 wt. %) and edges (27.46 wt. %) (Amin *et al.*, 2018). Our results are comparable to those of mammalian teeth enamel. The chemical elements present in the hooks are typical for acanthocephalans (Heckmann *et al.*, 2007, 2012).

On the other hand, all trunk spines of *C. australe* had the highest level of sulfur reaching 15.61 % in posterior spines, and negligible levels of calcium and phosphorous. The middle weaker transitional spines (Figs. 16, 23) had the lowest level of sulfur of only 5.97 %. These levels are characteristic of *C. australe* as the level of sulfur in the anterior and posterior spines of *Southwellina hispida* (Van Cleave, 1925) Witenberg, 1932 was only 0.98 % and 0.96 % and the levels of calcium and phosphorous was also negligible (Table 5 of Amin *et al.*, 2022a). In cystacanths of *Profillicollis altmani* (Perry, 1942) Van Cleave, 1947, another marine acanthocephalan, the pattern of sulfur levels in anterior, middle, and posterior spines was comparable to that in *C. australe* but the % weight was considerably lower (2.70 – 3.21 %, 2.56 %, and 3.28 – 3.94 %, respectively) and the % weight of phosphorous and calcium was considerably higher (Table 5, Amin *et al.*, 2022a). This comparison suggests that water salinity is not involved in the distribution of elements in the spines of marine species of acanthocephalans.

The acanthor of *C. australe* had much higher levels of metals, especially phosphorous (7.73 %) compared to the egg shells (0.91 %) (Table 4). In terrestrial acanthocephalans such as *Macracanthorhynchus hirudinaeus* (Pallas, 1781) infecting a mammalian host, *Sus scrofa* Linn., 1758, WT % of all metals, especially phosphorous was considerably higher in the cortical layer (23.48 %), compared to the middle of the egg (acanthor) (2.26 %), and moderate levels of sulfur and calcium (Table 3 in Amin *et al.*, 2021). Phosphorous is a basic element in the hardening of egg shell, especially of terrestrial acanthocephalans and may be related to the protection of eggs from desiccation. "The 4 outer eggshell layers E1–E4 surrounding the acanthor of *M. hirudinaeus* were shown to contain glycoproteins (Peters *et al.*, 1991). Glycoproteins are structural molecules forming collagen and some include phosphorus in phosphoserine (an ester of serine and phosphoric acid) in the process of P-glycosylation (Murray *et al.*, 2006) which may explain the high Phosphorous content of 23.48 % in the cortical eggshell layer only" (Amin *et al.*, 2021). "Results of X-ray scans of eggs are available in one other terrestrial species of acanthocephalans, *Centrorhynchus globocaudatus* (Zeder, 1800) Lühe, 1911 (Centrorhynchidae) were obtained from *Falco tinnunculus* Linn., 1758, (Falconidae) and *Buteo buteo* Linn., 1758 (Accipitridae) in northern Italy. Eggs of *C. globocaudatus* had the highest levels of sulfur in the cortical (12.94 %) and core areas (8.04 %) and a high level of Phosphorus (9.01 %) in the middle (Table 6, Fig. 32 in Amin *et al.*, 2020b).

X-ray scan analysis provides insight into the hardened components, e.g., calcium, sulfur, and phosphorus, of acanthocephalan hooks. The EDXA appears to be species-specific, as in fingerprints. For example, EDXA is shown to have significant diagnostic value in acanthocephalan systematics. For example, *Moniliformis cryptosaudi* Amin, Heckmann, Sharifdini, Albayati, 2019 from Iraq is morphologically identical to *Moniliformis saudi* Amin, Heckmann, Mohammed, Evans, 2016 from Saudi Arabia, and it was erected based primarily on its distinctly different EDXA pattern (Amin *et al.*, 2019) as a cryptic species. Our methodology for the detection of the chemical profile of hooks in the Acanthocephala has also been used in other parasitic groups including the Monogenea (Rubtsova *et al.*, 2018, Rubtsova & Heckmann, 2019) and Cestoda (Rubtsova & Heckmann, 2020).

Biological significance of EDXA

The taxonomic identity of species is deep-seated at the genetic level which is expressed by the organism's morphology and biochemistry as revealed, in part, by its elemental spectra. Amin *et al.* (2022a,b,c,d) discussed in detail the biological significance of EDXA as a diagnostic tool exemplified by the observation that populations of an acanthocephalan species will consistently have similar EDXA spectra irrespective of host species or geography. Metal analysis of hooks has become a diagnostic standard since hooks have the highest level of elements compared to the mid- and posterior trunk regions of the acanthocephalan body (Heckmann *et al.*, 2012).

Specifically, the Sulfur content in the proboscis is paramount in the composition of disulfide bonds in the thiol groups for cysteine and cystine of the polymerized protein molecules (Stegman, 2005). The formed disulfide bonds are direct by-products of the DNA-based process of protein synthesis which makes up the identity of a biological species. Accordingly, the level of sulfur in our EDXA profiles will indicate the number of sulfur bonds that along with the levels of calcium phosphates, will characterize the elemental identity of a species based on its nuclear DNA personality. Variations in chemical compositions probably indicate differences in allele expression. The DNA-generated sulfide bonds evident in our EDXA profiles have an important role in the stability and rigid nature of the protein accounting for the high sulfur content of the proboscis (Heckmann *et al.*, 2012). The above processes explain the observed species-specific nature of EDXA profiles noted in our many findings.

Molecular analysis

The present study contributes further continuation to the heteropolar geographical distribution for isolates of *C. australe* after the work of Lisitsyna *et al.* (2019) and García-Varela *et al.* (2021) having the novel information presented in the molecular study is the inclusion of *cox1* sequences of *C. australe* from Peru. In the present study, a total of two partial 18S and *Cox1* sequences were generated for *C. australe*. Newly generated 18S and *Cox1* sequences of *C. australe* were very similar and show low intraspecific genetic divergence. The sequence for *C. australe* of Lisitsyna *et al.* (2019) and García-Varela *et al.* (2021) from the USA and Mexico revealed a robust relationship with the present study isolates showing genetic divergence ranging between 0.9 to 1.0 %. This result suggests that the above sequence from the USA and Mexico in comparison with other populations of *C. australe* exhibited the lowest divergence level and that they all belong to the Northern Hemisphere. Genetic divergence among the current study population with isolates from the Southern Hemisphere ranged from 1.8 to 3.0 %. The systematic position of the *C. australe* isolates in the phylogenetic tree strongly suggested that the isolates fit the similar evolutionary lineage and follow the same pattern in the haplotype network (Figs. 42 and 43). For that reason, molecular data used in the studies of acanthocephalans will make available valuable information about their diversity and population studies. Our study represents the new isolates clustered together, and displayed shared haplotypes, with isolates sequenced by Lisitsyna *et al.* (2019) and García-Varela *et al.* (2021). The haplotype network in the current study was constructed using *Cox1* sequences of 46 specimens of *C. australe* from North and South American countries. The 46 sequences of *C. australe* were collapsed into 22 haplotypes and our haplotype network strongly comprised two clusters based in the Northern and Southern Hemispheres. The first (I) group related to the population of *C. australe* from North America that includes specimens from the USA and Mexico and the study of García-Varela *et al.* (2021) also supports the present analysis.

The second (II) group resembled populations from South America that comprises specimens from Peru, Argentina and Brazil. These data, in association with the phylogeny evidence, support the distinct population status of *C. australe*. Though, the distribution of specimens of *C. australe* population from different regions was in consensus in representing species group at the genetic level (Figs. 42 and 43). The newly generated sequences in the present study clustered within the first (I) group clade representing species of the USA and Mexico while the specimens from Peru, Argentina and Brazil appeared associated with the second (II) group clade and these relationships were also supported by the previous study of García-Varela *et al.* (2021).

In the present study, molecular data clearly represented the wide distribution of a single species that might be the leading step in further understanding the speciation and evolution of this species in the future.

Acknowledgements

This project was supported by the Department of Biology, Brigham Young University (BYU), Provo, Utah, and by an Institutional Grant from the Parasitology Center, Inc. (PCI), Scottsdale, Arizona. The EDXA and SEM methodologies used in this project have been pioneered by Dr. Richard A. Heckmann (deceased) (BYU) to whom we shall always dedicate our highest gratitude. We thank Madison Laurence and Elisabeth Trimble, Bean Museum (BYU) and Dr. Nataliya Rubtsova (PCI) for expert help in the preparation and organization of plates and figures. We are also grateful to Michael Standing, Electron Optics Laboratory (BYU), for his technical help and expertise with the preparation of the SEM images and the generation of the EDXA data. The authors thank the head of the Department of Zoology, Chaudhary Charan Singh University, Meerut, India for providing laboratory facilities. The authors declare conflicts of interest none.

Conflict of Interest

The authors declare no conflicts of interest.

References

AMIN, O.M. (2013): Classification of the Acanthocephala. *Folia Parasitol*, 60: 273 – 305. DOI: 10.14411/fp.2013.031

AMIN, O.M., HECKMANN, R.A., RADWAN, N.A., MANTUANO, J.S., ALCIVAR, M.A.Z. (2009): Redescription of *Rhadinorhynchus ornatus* (Acanthocephala: Rhadinorhynchidae) from skipjack tuna, *Katsuwonus pelamis*, collected in the Pacific Ocean off South America, with special reference to new morphological features. *J Parasitol*, 95: 656 – 664. DOI: 10.1645/GE-1804.1

AMIN, O.M., HECKMANN, R.A., HALAJIAN, A., EL-NAGGAR, A.M. (2011): The morphology of an unique population of *Corynosoma strumosum* (Acanthocephala, Polymorphidae) from the Caspian seal,

Pusa caspica, in the land-locked Caspian Sea using SEM, with special notes on histopathology. *Acta Parasitol*, 56: 438 – 445. DOI: 10.2478/s11686-011-0070-6

AMIN, O.M., HECKMANN, R.A., BANNAI, M.A. (2018): *Cavisoma magnum* (Cavisomidae), a unique Pacific acanthocephalan re-described from an unusual host, *Mugil cephalus* (Mugilidae), in the Arabian Gulf, with notes on histopathology and metal analysis. *Parasite*, 25: 5. DOI: 10.1051/parasite/2018006

AMIN, O.M., HECKMANN, R.A., SHARIFDINI, M., ALBAYATI, N.Y. (2019): *Moniliformis cryptosaudi* n. sp. (Acanthocephala: Moniliformidae) from the Long-eared Hedgehog *Hemiechinus auritus* (Gmelin) (Erinaceidae) in Iraq; A Case of Incipient Cryptic Speciation Related to *M. saudi* in Saudi Arabia. *Acta Parasitol*, 64: 195 – 204. DOI: 10.2478/s11686-018-00021-9

AMIN, O.M., RUBTSOVA, N., HECKMANN, R.A. (2020a): Accessory copulatory structures in the bursa of male acanthocephalans. *Sci Parasitol*, 21: 102 – 119

AMIN, O.M., HECKMANN, R.A., DALLARÉS, S., CONSTENLA, M., RUBINI, S. (2020b): Description and molecular analysis of an Italian population of *Centrorhynchus globocaudatus* (Zeder, 1800) Lühe, 1911 (Acanthocephala: Centrorhynchidae) from *Falco tinnunculus* (Falconidae) and *Buteo buteo* (Accipitridae). *J. Helminthol*, 94: 1 – 21. DOI: 10.1017/S0022149X20000887

AMIN, O.M., HECKMANN, R.A., DALLARÉS, S., CONSTENLA, M., KUZMINA, T. (2021): New morphological and molecular perspectives about *Macracanthorhynchus hirudinaceus* (Acanthocephala: Oligacanthorhynchidae) from wild boar, *Sus scrofa* Linn., in Ukraine. *J Helminthol*, 95: 1 – 11. DOI: 10.1017/S0022149X21000675

AMIN, O.M., CHAUDHARY, A., SINGH, H.S. (2022a): Description of immature *Southwellina hispida* (Van Cleave, 1925) Witenberg, 1932 (Acanthocephala: Polymorphidae) from the body cavity of the paratenic host *Gillichthys mirabilis* Cooper (Gobiidae) in California. *Acta Parasitol*, DOI:10.1007/s11686-022-00552-2

AMIN, O.M., AHMED, M., CHAUDHARY, A., HECKMANN, R.A., SINGH, H.S. (2022b): The morphological and molecular description of *Neoechinorhynchus* (*Neoechinorhynchus*) *poonchensis* n. sp. from *Schizothorax richardsonii* (Gray) in Poonch, Jammu and Kashmir, India. *Folia Parasitol*, 69: 001. DOI: 10.14411/fp.2022.001

AMIN, O.M., LISITSYNA, O., HECKMANN, R.A. (2022c): Evaluating energy dispersive X-ray analysis (EDXA) as a diagnostic tool in acanthocephalan taxonomy as evidenced in Palaeacanthocephala and Archiacanthocephala. *Syst Parasitol*, 100: 43 – 57. DOI: 10.1007/s11230-022-10069-x

AMIN, O.M., RODRÍGUEZ, S.M., RUBTSOVA, N., HECKMANN, R.A., PEÑA, C., CASTRO, T., RIVERA, F., D'ELIA, G. (2022d): A comparative assessment of the morphology of *Profillicollis altmani* (Acanthocephala, Polymorphidae) from crustaceans and shore birds in Peru, with special notes on hook elemental analysis (EDXA), SEM imaging, histopathology, and molecular profile. *Parasite*, 29: 9. DOI: 10.1051/parasite/2022005

ANGLADE, T., RANDHAWA, H.S. (2018): Gaining insights into the ecological role of the New Zealand sole (*Peltorhamphus novaezee-*

- landiae*) through parasites. *J Helminthol*, 92(2): 187 – 196. DOI: 10.1017/S0022149X17000323
- AZNAR, F.J., PEREZ-PONCE DE LEÓN, G., RAGA, J.A. (2006): Status of *Corynosoma* (Acanthocephala: Polymorphidae) based on anatomical, ecological and phylogenetic evidence, with the erection of *Pseudocorynosoma* n. gen. *J Parasitol*, 92: 548 – 564. DOI: 10.1645/GE-715R.1
- AZNAR, F.J., HERNÁNDEZ-ORTS, J., SUÁREZ, A.A., GARCÍA-VARELA, M., RAGA, J.A., CAPPOZZO, H.L. (2012): Assessing host-parasite specificity through coprological analysis: a case study with species of *Corynosoma* (Acanthocephala: Polymorphidae) from marine mammals. *J Helminthol*, 86: 156 – 164. DOI: 10.1017/S0022149X11000149
- AZNAR, F.J., CRESPO, E.A., REGA, J.A., HERNÁNDEZ-ORTS, J.S. (2016): Trunk spines in cystacanths and adults of *Corynosoma* spp. (Acanthocephala): *Corynosoma cetaceum* as an exceptional case of phenotypic variability. *Zoomorphology*, 135: 19 – 31. DOI: 10.1007/s00435-015-0290-7
- BANDELT, H.J., FORSTER, P., RÖHL, A. (1999): Median-joining networks for inferring intraspecific phylogenies. *Mol Biol Evol*, 16: 37 – 48. DOI: 10.1093/oxfordjournals.molbev.a026036
- BYRAM, J.E., FISHER JR, F.M. (1973): The absorptive surface of *Moniliformis dubius* (Acanthocephala). 1. Fine structure. *Tissue Cell*, 5: 553 – 579. DOI: 10.1016/S0040-8166(73)80045-X
- FOLMER, O., BLACK, M., HOEH, W., LUTZ, R., VRIJENHOEK, R. (1994): DNA primers for amplification of mitochondrial cytochrome c oxidase subunit I from diverse metazoan invertebrates. *Mol Marine Biol Biotechnol*, 3: 294 – 299
- FONSECA, M.C.G.D., KNOFF, M., FELIZARDO, N.N., TORRES, E.J.L., DI AZEVEDO, M.I.N., GOMES, D.C., CLEMENTE, S.C.S., INÍGUEZ, A.M. (2019): Acanthocephalan parasites of the flounder species *Paralichthys isosceles*, *Paralichthys patagonicus* and *Xystreurys rasile* from Brazil. *Rev Bras Parasitol Vet*, 28(3): 346 – 359. DOI: 10.1590/S1984-29612019031
- GARCÍA-VARELA, M., NADLER, S.A. (2006): Phylogenetic relationships among Syndermata inferred from nuclear and mitochondrial gene sequences. *Mol Phylogenet Evol*, 40(1): 61 – 72. DOI: 10.1016/j.ympev.2006.02.010
- GARCÍA-VARELA, M., PÉREZ-PONCE DE LEÓN, G. (2008): Validating the systematic position of *Profillicollis* Meyer, 1931 and *Hexaglandula* Petrochenko, 1950 (Acanthocephala: Polymorphidae) using cytochrome c oxidase (Cox 1). *J Parasitol*, 94(1): 212 – 217. DOI: 10.1645/GE-1257.1
- GARCÍA-VARELA, M., PEREZ-PONCE DE LEÓN, G., AZNAR, F.J., NADLER, S.A. (2009): Systematic position of *Pseudocorynosoma* and *Andracantha* (Acanthocephala, Polymorphidae) based on nuclear and mitochondrial gene sequences. *J Parasitol*, 95: 178 – 185. DOI: 10.1645/GE-1538.1
- GARCÍA-VARELA, M., PEREZ-PONCE DE LEÓN, G., AZNAR, F.J., NADLER, S.A. (2013): Phylogenetic relationship among genera of Polymorphidae (Acanthocephala), inferred from nuclear and mitochondrial gene sequences. *Mol Phylogenet Evol*, 68 (2): 176 – 184. DOI: 10.1016/j.ympev.2013.03.029
- GARCÍA-VARELA, M., HENANDEZ-ORTS, J.S., PINACHO-PINACHO, C.D. (2017): A morphological and molecular study of *Pseudocorynosoma* Aznar, Perez Ponce de Leon and Raga 2006 (Acanthocephala: Polymorphidae) from Mexico with the description of a new species and the presence of cox 1 pseudogenes. *Parasitol Int*, 66(2): 27 – 36. DOI: 10.1016/j.parint.2016.11.007
- GARCÍA-VARELA, M., MASPER, A., CRESPO, E.A., HERNANDEZ-ORTS, J.S. (2021): Genetic diversity and phylogeography of *Corynosoma australe* Johnston, 1937 (Acanthocephala: Polymorphidae), an endoparasite of otariids from the Americas in the northern and southern hemispheres. *Parasitol Int*, 80: 102205. DOI: 10.1016/j.parint.2020.102205
- GIBSON, D., WAYLAND, M. (2022): *World List of marine Acanthocephala*. *Corynosoma obtuscens* Lincicome, 1943. Accessed through: World Register of Marine Species at: <https://www.marinespecies.org/aphia.php?p=taxdetails&id=448864> on 2022-01-14.
- GUILLÉN-HERNÁNDEZ, S., GARCÍA-VARELA, M., LEÓN, G.P.D. (2008): First record of *Hexaglandula corynosoma* (Travassos, 1915) Petrochenko, 1958 (Acanthocephala: Polymorphidae) in intermediate and definitive hosts in Mexico. *Zootaxa*, 1873: 61 – 68. DOI: 10.5281/zenodo.184057
- HALAJIAN, A., SMALES, L., HECKMANN, R., AMAKALI, A.M., TJIPUTE, M., WILHELM, M.R., LUIUS POWELL, W.J. (2020): *Corynosoma australe* and *Bolbosoma vasculosum* (Polymorphidae: Acanthocephala) from *Arctocephalus pusillus pusillus* (Otariidae) and *Argyrosomus* spp. (Sciaenidae) from the Namibian coast of Africa. *Comp Parasitol*, 87: 124 – 131. DOI: 10.1654/1525-2647-87.1.127
- HALL, T.A. (1999): BioEdit: A User-Friendly Biological Sequence Alignment Editor and Analysis Program for Windows 95/98/NT. *Nucleic Acids Symp Ser (Oxf)*, 41: 95 – 98. DOI: 10.12691/ajmr-2-6-8
- HECKMANN, R.A. (2006): Energy dispersive x-ray analysis (EDXA) in conjunction with electron optics, a tool for analyzing aquatic animal parasite diseases and deaths, an update. *Proc Parasitol*, 41: 1 – 18
- HECKMANN, R.A., AMIN, O.M., STANDING, M.D. (2007): Chemical analysis of metals in Acanthocephalans using energy dispersive X-ray analysis (EDXA, XEDS) in conjunction with a scanning electron microscope (SEM). *Comp Parasitol*, 74: 388 – 391. DOI: 10.1654/4258.1
- HECKMANN, R.A., AMIN, O.M., RADWAN, N.A.E., STANDING, M.D., EGGETT, D.L. EL NAGGAR, A.M. (2012): Fine structure and energy dispersive X-ray analysis (EDXA) of the proboscis hooks of *Radionorynchus ornatus*, Van Cleave 1918 (Rhadinorynchidae: Acanthocephala). *Sci Parasitol*, 13: 37 – 43
- HECKMANN, R.A., AMIN, O.M., EL NAGGAR, A.M. (2013): Micropores of Acanthocephala, a scanning electron microscopy study. *Sci Parasitol*, 14: 105 – 113
- HERNÁNDEZ-ORTS, J.S., BRANDÃO, M., GEORGIEVA, S., RAGA, J.A., CRESPO, E.A., LUQUE, J.L. AZNAR, F.J. (2017a): From mammals back to birds: Host-switch of the acanthocephalan *Corynosoma australe*

- from pinnipeds to the Magellanic penguin *Spheniscus magellanicus*. *PLoS One*, 12: e0183809. DOI: 10.1371/journal.pone.0183809
- HERNÁNDEZ-ORTS, J.S., SMALES, L.R., PINACHO-PINACHO, C.D., GARCÍA-VARELA, M., PRESSWELL, B. (2017b): Novel morphological and molecular data for *Corynosoma hanna* Zdzitowiecki, 1984 (Acanthocephala: Polymorphidae) from teleosts, fish-eating birds and pinnipeds from New Zealand. *Parasitol Int*, 66: 905 – 916. DOI: 10.1016/j.parint.2016.10.007
- HERNÁNDEZ-ORTS, J.S., HERNÁNDEZ-MENA, D.I., PANTOJAMILA, C., KUČHTA, R., GARCÍA, N.A., CRESPO, E.A., LOIZAGA, R. (2021): A Visitor of Tropical Waters: First Record of a Clymene Dolphin (*Stenella clymene*) Off the Patagonian Coast of Argentina, With Comments on Diet and Metazoan Parasites. *Front Mar Sci*, 8: 658975. DOI: 10.3389/fmars.2021.658975
- JOHNSTON, T.H. (1937): Entozoa from the Australian hair seal. *Proc Linn Soc N S W*, 62: 9 – 16
- JOHNSTON, T.H., EDMONDS, S.J. (1953): Acanthocephala from Auckland and Campbell Islands. *Dom Mus. Rec. Zool.*, 2: 55 – 61
- KUZMINA, T.A., SPRAKER, T.R., KUDLAI, O., LISITSYNA, O.I., ZABLUDOVSKAJA, S.O., KARBOWIAK, G., FONTAINE, C., KUČHTA, R. (2018): Metazoan parasites of California sea lions (*Zalophus californianus*): A new data and review. *Int J Parasitol Parasites Wildl*, 7(3): 326 – 334. DOI: 10.1016/j.ijppaw.2018.09.001
- LEE, R.E. (1992): *Scanning electron microscopy and X-ray microanalysis*. Prentice Hall, Englewood Cliffs, New Jersey, 464 pp.
- LEVY, E., ROSSIN, M.A., BRAICOVICH, P.E., TIMI, J.T. (2020): *Proflicolilis chasmagnathi* (Acanthocephala) parasitizing freshwater fishes: paratenicity and an exception to the phylogenetic conservatism of the genus? *Parasitol Res*, 119(12): 3957 – 3966. DOI: 10.1007/s00436-020-06825-x
- LIBRADO, P., ROZAS, J. (2009): DnaSP v5: a software for comprehensive analysis of DNA polymorphism data. *Bioinformatics*, 25: 1451 – 1452. DOI: 10.1093/bioinformatics/btp187
- LINCICOME, D.R. (1943): Acanthocephala of the genus *Corynosoma* from the California sea lion. *J Parasitol*, 29: 102 – 106
- LISITSYNA, O.I., KUDLAI, O., SPRAKER, T.R., KUZMINA, T.A. (2018): New records on acanthocephalans from California sea lions *Zalophus californianus* (Pinnipedia: Otariidae) from California, USA. *Vestn Zool*, 52: 181 – 192. DOI: 10.2478/vzoo-2018-0019
- LISITSYNA, O.I., KUDLAI, O., SPRAKER, T.R., TKACH, V.A., SMALES, L.R., KUZMINA, T.A. (2019): Morphological and molecular evidence for synonymy of *Corynosoma obtuscens* Lincicome, 1943 with *Corynosoma australe* Johnston, 1937 (Acanthocephala: Polymorphidae). *Sys Parasitol*, 96: 95 – 110. DOI: 10.1007/s11230-018-9830-0
- MILNE, I., LINDNER, D., BAYER, M., HUSMEIER, D., MCGUIRE, G., MARSHALL, D.F., WRIGHT, F. (2009): TOPALiv2: A rich graphical interface for evolutionary analyses of multiple alignments on HPC clusters and multi-core desktops. *Bioinformatics*, 25: 126 – 127. DOI: 10.1093/bioinformatics/btn575
- MORINI, E.G., BOERO, J.J. (1960): *Corynosoma otariae* n. sp. (Acanthocephala; Polymorphidae) parasito de un lobo marino (*Otaria flavescens*) [*Corynosoma otariae* n. sp. (Acanthocephala; Polymorphidae) parasite of a sea lion (*Otaria flavescens*)]. In: *Actas y Trabajos 1 Congreso Sudamericano de Zoología II* (La Plata, 1959) [*Proceedings and Works 1 South American Congress of Zoology II*], 229 – 234 (In Spanish)
- MURRAY, R.K., GRANNER, D.K., RODWELL, V.W. (2006): *Harper's Illustrated Biochemistry*. 27th Edition, McGraw-Hill, 672 pp.
- NEAR, T.J., GAREY, J.R., NADLER, S.A. (1998). Phylogenetic relationships of the Acanthocephala inferred from 18S ribosomal DNA sequences. *Mol Phylogenet Evol*, 10 (3), 287 – 298. DOI: 10.1006/mpev.1998.0569
- PETERS, W., TARASCHEWSKI, H., LATKA, I. (1991): Comparative investigations of the morphology and chemical composition of the eggshells of Acanthocephala. I. *Macracanthorhynchus hirudinaeus* (Archiacanthocephala). *Parasitol Res*, 77: 542 – 549. DOI: 10.1007/BF00928424
- RUBTSOVA, N.Y., HECKMANN, R.A. (2019): Structure and morphometrics of *Ancyrocephalus paradoxus* (Monogenea: Ancyrocephalidae) from *Sander lucioperca* (Percidae) in Czechia. *Helminthologia*, 56: 11 – 21. DOI: 10.2478/helm-2018-0037
- RUBTSOVA, N.Y., HECKMANN, R.A. (2020): Morphological features and structural analysis of plerocercoids of *Spirometra erinaceieuropaei* (Cestoda: Diphyllbothriidae) from European pine marten, *Martes martes* (Mammalia: Mustelidae) in Ukraine. *Comp Parasitol*, 87: 109 – 117. DOI: 10.1654/1525-2647-87.1.109
- RUBTSOVA, N.Y., HECKMANN, R.A., SMIT, W.S., LUUS-POWELL, W.J., HALAJIAN, A., ROUX, F. (2018): Morphological studies of developmental stages of *Oculotrema hippopotami* (Monogenea: Polystomatidae) infecting the eye of *Hippopotamus amphibius* (Mammalia: Hippopotamidae) using SEM and EDXA with notes on histopathology. *Korean J Parasitol*, 56: 463 – 475. DOI: 10.3347/kjp.2018.56.5.463
- SANTORO, M., PALOMBA, M., GILI, C., MARCER, F., MARCHIORI, E., MATTIUCCI, S. (2021): Molecular and morphological characterization of *Bolbosoma balaenae* (Acanthocephala: Polymorphidae), a neglected intestinal parasite of the fin whale *Balaenoptera physalus*. *Parasitology*, 148(11): 1293 – 1302. DOI: 10.1017/S0031182021000925
- SARDELLA, N.H., MATTIUCCI, S., TIMI, J.T., BASTIDA, R.O., RODRIGUEZ, D.H., NASCETTI, G. (2005): *Corynosoma australe* Johnston, 1937 and *C. cetaceum* Johnston & Best, 1942 (Acanthocephala: Polymorphidae) from marine mammals and fishes in Argentinian waters: allozyme markers and taxonomic status. *Syst Parasitol*, 61: 143 – 156. DOI: 10.1007/s11230-005-3131-0
- SMALES, L.R. (1986): Polymorphidae (Acanthocephala) from Australian mammals with description of two new species. *Syst Parasitol*, 8: 91 – 100. DOI: 10.1007/BF00009865
- STANDING, M.D., HECKMANN, R.A. (2014): Features of Acanthocephalan hooks using dual beam preparation and XEDS phase maps. In *Microscopy and Microanalysis Meeting, Hartford, Connecticut, U.S.A.* Poster. Submission Number 0383–00501
- STEGMAN, J.K. (2005): *Stedman's Medical Dictionary for the Health Professions and Nursing*. 5th Edition. Lippincott, Williams and

- Wilkins, Baltimore, Maryland, USA, 1597 pp.
- STRYUKOV, A.A. (2004): Infection of true seals in Antarctica with acanthocephalans. *Vestn Zool*, 38(4): 23 – 29 (In Russian)
- SUZUKI, N., HOSHINO, K., MURAKAMI, K., TAKEYAMA, H., CHOW, S. (2008): Molecular diet analysis of *Phyllosoma* larvae of the Japanese spiny lobster *Palinurus japonicus* (Decapoda: Crustacea). *Mar Biotechnol*, 10: 49 – 55. DOI: 10.1007/s10126-007-9038-9
- TAMURA, K., GLEN, S., KUMAR, S. (2021): MEGA11: Molecular Evolutionary Genetics Analysis Version 11. *Mol Biol Evol*, 38: 3022 – 3027. DOI: 10.1093/molbev/msab120
- VAN CLEAVE, H.J. (1953): *Acanthocephala of North American mammals*. Illinois Biological Monographs 23, 179 pp.
- VERWEYEN, L., KLIMPEL, S., PALM, H.W. (2011): Molecular phylogeny of the Acanthocephala (class Palaeacanthocephala) with a paraphyletic assemblage of the orders Polymorphida and Echinorhynchida. *PLoS One*, 6(12): E28285. DOI: 10.1371/journal.pone.0028285
- WAINDOK P, LEHNERT K, SIEBERT U, PAWLICZKA I, STRUBE C. (2018): Prevalence and molecular characterisation of Acanthocephala in pinnipedia of the North and Baltic Seas. *Int J Parasitol Parasites Wildl*, 7(1): 34 – 43. DOI: 10.1016/j.ijppaw.2018.01.002
- WHITFIELD, P.J. (1979): *The biology of parasitism: An introduction to the study of associating organisms*. University Park Press, Baltimore, Maryland, 277 pp.
- WRIGHT, R.D., LUMSDEN, R.D. (1969): Ultrastructure of the tegumentary pore-canal system of the acanthocephalan *Moniliformis dubius*. *J Parasitol*, 55: 993 – 1003
- ZDZITOWIECKI, K. (1984): Some Antarctic acanthocephalans of the genus *Corynosoma* parasitizing Pinnipedia, with descriptions of three new species. *Acta Parasitol Pol*, 29: 359 – 377
- ZDZITOWIECKI, K. (1991): Antarctic Acanthocephala. In: WÄGELE, J.W., SIEG, J. (Eds) *Synopses of the Antarctic Benthos*. Volume 3 Koenigstein Koeltz Scientific Books, Polish Academy of Sciences, Warszawa, 116 pp.